# Part A
# Fundamental Nuclear Research



*Encyclopedia of Nuclear Physics and its Applications,* First Edition. Edited by Reinhard Stock.

# 1
# Nuclear Structure

*Jan Jolie*



*Encyclopedia of Nuclear Physics and its Applications*, First Edition. Edited by Reinhard Stock.

## 1.1 Introduction

The study of nuclear structure today encompasses a vast territory from the study of simple, few-particle systems to systems with close to 300 particles, from stable nuclei to the short-lived exotic nuclei, from ground-state properties to excitations of such energy that the nucleus disintegrates into substructures and individual constituents, from the strong force that hold the atomic nucleus together to the effective interactions that describe the collective behavior observed in many heavy nuclei.

After the discovery of different kinds of radioactive decays, the discovery of the structure of the atomic nucleus begins with the fundamental paper by Ernest Rutherford [1], in which he explained the large-angle alpha (α)-particle scattering from gold that had been discovered earlier by Hans W. Geiger and Ernest Marsden. Indeed, Rutherford shows that the atom holds in its center a very tiny, positively charged nucleus that contains 99.98% of the atomic mass. In 1914, Henry Moseley [2, 3] showed that the nuclear charge number $Z$ equaled the atomic number. Using the first mass separators, Soddy [4] was able to show that one chemical element could contain atomic nuclei with different masses, forming different isotopes. With the availability of α-sources, due to the works of the Curies in Paris, Rutherford [5] was able to perform the first nuclear reactions on nitrogen. The first attempt at understanding the relative stability of nuclear systems was made by Harkins and Majorsky [6]. This model, like many others of the time, consisted of protons and electrons. In 1924, Wolfgang Pauli [7] suggested that the optical hyperfine structure might be explained if the nucleus had a magnetic dipole moment, while later Giulio Racah [8] investigated the effect on the hyperfine structure if the nuclear charge were not spherically symmetric – that is, if it had an electric quadrupole moment.

All of these structure suggestions occurred before James Chadwick [9] discovered the neutron, which not only explained certain difficulties of previous models (e.g., the problems of the confinement of the electron or the spins of light nuclei), but opened the way to a very rapid expansion of our knowledge of the structure of the nucleus. Shortly after the discovery of the neutron, Heisenberg [10] proposed that the proton and neutron are two states of the nucleon classified by a new spin quantum number, the isospin. It may be difficult to believe today, 60 years after Chadwick's discovery, just how rapidly our knowledge of the nucleus increased in the mid-1930s.

*Encyclopedia of Nuclear Physics and its Applications*, First Edition. Edited by Reinhard Stock.

Hans A. Bethe's review articles [11, 12], one of the earliest and certainly the best known, discuss many of the areas that not only form the basis of our current knowledge but that are still being investigated, albeit with much more sophisticated methods.

The organization here will begin with general nuclear properties, such as size, charge, and mass for the stable nuclei, as well as half-lives and decay modes (α, β, γ, and fission) for unstable systems. Binding energies and the mass defect lead to a discussion of the stability of systems and the possibility of nuclear fusion and fission. Then follow details of the charge and current distributions, which, in turn, lead to an understanding of static electromagnetic moments (magnetic dipole and octupole, electric quadrupole, etc.) and transitions. Next follows the discussion of single-particle and collective levels for the three classes of nuclei: even–even, odd-*A*, and odd–odd (i.e., odd *Z* and odd *N*). With these mainly experimental details in hand, a discussion of various major nuclear models follows. These discussions attempt, in their own way, to categorize and explain the mass of experimental data.

## 1.2 General Nuclear Properties

### 1.2.1 Properties of Stable Nuclei

The discovery of the neutron allowed each nucleus to be assigned a number, *A*, the mass number, which is the sum of the number of protons (*Z*) and neutrons (*N*) in the particular nucleus. The atomic number of chemistry is identical to the proton number *Z*. The mass number *A* is the integer closest to the ratio between the mass of a nucleus and the fundamental mass unit. This mass unit, the unified atomic mass unit, has the value $1\ \mathrm{u} = 1.660538921(73) \times 10^{-27}\ \mathrm{kg} = 931.494061(21)\ \mathrm{MeV\,c^{-2}}$. It has been picked so that the atomic mass of a $^{12}C_6$ atom is exactly equal to 12 u. The notation here is $^{A}X_{N}$, where X is the chemical symbol for the given element, which fixes the number of electrons and hence the number of protons *Z*. This commonly used notation contains some redundancy because $A = Z + N$ but avoids the need for one to look up the *Z*-value for each chemical element. From this last expression, one can see that there may be several combinations of *Z* and *N* to yield the same *A*. These nuclides are called *isobars*. An example might be the pair $^{196}Pt_{118}$ and $^{196}Au_{117}$. Furthermore, an examination of a table of nuclides shows many examples of nuclei with the same *Z*-value but different *A*- and *N*-values. Such nuclei are said to be *isotopes* of the element. For example, oxygen (O) has three stable isotopes: $^{16}O_8$, $^{17}O_9$, and $^{18}O_{10}$. A group of nuclei that have the same number of neutrons, *N*, but different numbers of protons, *Z* (and, of course, *A*), are called *isotones*. An example might be $^{38}Ar_{20}$, $^{39}K_{20}$, and $^{40}Ca_{20}$. Some elements have but one stable isotope (e.g., $^{9}Be_5$, $^{19}F_{10}$, and $^{197}Au_{118}$), others, two, three, or more. Tin ($Z = 50$) has the most at 10. Finally, the element technetium has no stable isotope at all. A final definition of use for light nuclei is a *mirror pair*, which is a pair of nuclei with *N* and *Z* interchanged. An example of such a pair would be $^{23}Na_{12}$ and $^{23}Mg_{11}$.

The nuclear masses of stable isotopes are determined with a mass spectrometer, and we shall return to this fundamental property when we discuss the nuclear binding energy and the mass defect in Section 1.3. After mass, the next property

of interest is the size of a nucleus. The simplest assumption here is that the mass and charge form a uniform sphere whose size is determined by the radius. While not all nuclei are spherical or of uniform density, the assumption of a uniform mass/charge density and spherical shape is an adequate starting assumption (more complicated charge distributions are discussed in Section 1.4 and beyond). The nuclear radius and, therefore, the nuclear volume or size is usually determined by electron-scattering experiments; the radius is given by the relation

$$R = r_0 A^{1/3} \tag{1.1}$$

which, with $r_0 = 1.25$ fm, gives an adequate fit over the entire range of nuclei near stability. An expression such as Eq. (1.1) implies that nuclei have a density independent of $A$, that is, they are incompressible. A somewhat better fit to the nuclear sizes can be obtained from the Coulomb energy difference of mirror nuclei, which covers but a fifth of the total range of $A$. This yields $r_0 = 1.22$ fm. Even if the charge and/or mass distribution is neither spherical nor uniform, one can still define an equivalent radius as a size parameter.

Two important properties of a nuclide are the spin $J$ and the parity $\pi$, often expressed jointly as $J^\pi$, of its ground state. These are usually listed in a table of isotopes and give important information about the structure of the nuclide of interest. An examination of such a table will show that the ground state and parity of all even–even nuclei is $0^+$. The spin and parity assignments of the odd-$A$ and odd–odd nuclei tell a great deal about the nature of the principal parts of their ground-state wave functions. A final property of a given element is the relative abundance of its stable isotopes. These are determined again with a mass spectrograph and listed in various tables of the nuclides.

### 1.2.2 Properties of Radioactive Nuclei

A nucleus that is unstable, that is, it can decay to a different or *daughter* nucleus, is characterized not only by its mass, size, spin, and parity but also by its lifetime $\tau$ and decay mode or modes. (In fact, each level of a nucleus is characterized by its spin, parity, lifetime, and decay modes.) The law of radioactive decay is simply

$$N(t) = N(0)e^{-\lambda t} = N(0)e^{-t/\tau} \tag{1.2}$$

where $N(0)$ is the number of nuclei initially present, $\lambda$ is the decay constant, and its reciprocal $\tau$ is the lifetime. Instead of the lifetime, often the half-life $T_{1/2}$ is used. It is the time in which half of the nuclei decay. By setting $N(T_{1/2}) = N(0)/2$ in Eq. (1.2), one obtains the relation

$$T_{1/2} = \ln(2)\tau = 0.693\tau \tag{1.3}$$

The decay mode of ground states can be α, β, or spontaneous fission. Excited states mostly decay by γ-emission. More exotic decays are observed in unstable nuclei far from stability where nuclei decay takes place by emission of a proton or neutron.

In α-decay, the parent nucleus emits an α-particle (a nucleus of $^4He_2$), leaving the daughter with two fewer neutrons and protons:

$$^A X_N \rightarrow {}^{A-4}Y_{N-2} + {}^4He_2 \tag{1.4}$$

The α-particle has zero spin, but it can carry off angular momentum. In β-decay the weak interaction converts neutrons into protons ($\beta^-$-decay) or protons into neutrons ($\beta^+$-decay). Which of the two

decays takes place depends strongly on the masses of the initial and final nuclei. Because a neutron is heavier than a proton, the free neutron is unstable against $\beta^-$-decay and has a lifetime of 878.5(10) s. The mass excess in $\beta^-$-decay is released as kinetic energy of the final particles. In the case of the free neutron, the final particles are a proton, an electron, and an antineutrino, denoted by $\overline{\nu}$. All of these particles have spin 1/2 and can also carry off angular momentum. In the case of $\beta^+$-decay, the final particles are a bound proton, an antielectron or positron, and a neutrino. Finally, as an alternative to $\beta^+$-decay the initial nucleus can capture an inner electron. In this so-called electron capture decay, only a neutrino, $\nu$, is emitted by the final nucleus. In general, the decays can be written as

$$\beta^-\text{-decay}: \quad {}^{A}\mathrm{X}_N \rightarrow {}^{A}\mathrm{Y}_{N-1} + \mathrm{e}^- + \overline{\nu} \quad (1.5a)$$

$$\beta^+\text{-decay}: \quad {}^{A}\mathrm{X}_N \rightarrow {}^{A}\mathrm{Y}_{N+1} + \mathrm{e}^+ + \nu \quad (1.5b)$$

$$\beta^+\text{-decay (ec)}: \quad {}^{A}\mathrm{X}_N + \mathrm{e}^- \rightarrow {}^{A}\mathrm{Y}_{N-1} + \nu \quad (1.5c)$$

One very rare mode of decay is double β-decay, in which a nucleus is unable to β-decay to a $Z+1$ daughter for energy reasons but can emit two electrons and make a transition to a $Z+2$ daughter. An example is ${}^{82}\mathrm{Se}_{48} \rightarrow {}^{82}\mathrm{Kr}_{46}$ with a half-life of $(1.7 \pm 0.3) \times 10^{20}$ years. Double β-decay is observed under the emission of two neutrinos. Neutrinoless double β-decay is intensively searched for in ${}^{76}$Ge because it is forbidden for massless neutrinos with definite helicities. Enriched Ge is hence used as it allows the use of a large single crystal as source and detector (for a review see [13]).

In spontaneous fission, a very heavy nucleus simply breaks into two heavy pieces. For a given nuclide, the decay mode is not necessarily unique. If more than one mode occurs, then the branching ratio is also a characteristic of the radioactive nucleus in question.

An interesting example of a multimode radioactive nucleus is ${}^{242}\mathrm{Am}_{147}$. Its ground state ($J^\pi = 1^-$, $T_{1/2} = 16.01$ h) can decay either by electron capture (17.3% of the time) to ${}^{242}\mathrm{Pu}_{148}$ or by $\beta^-$ decay (82.7% of the time) to ${}^{242}\mathrm{Cm}_{146}$. On the other hand, a low-lying excited state at 0.04863 MeV ($J^\pi = 5^-$, $T_{1/2} = 152$ years) can decay either by emitting a γ-ray (99.52% of the time) and going to the ground state or by emitting an α-particle (0.48% of the time) and going to ${}^{238}\mathrm{Np}_{145}$. There is an excited state at 2.3 MeV with a half-life of 14.0 ms that undergoes spontaneous fission [14]. The overall measured half-life of ${}^{242}\mathrm{Am}_{147}$ is then determined by that of the 0.04863 MeV state. Such long-lived excited states are known as *isomeric states*. From this information on branching ratios, one easily finds the several partial decay constants for ${}^{242}\mathrm{Am}_{147}$. For the ground state, $\lambda_{\mathrm{ec}} = 2.080 \times 10^{-6}\ \mathrm{s}^{-1}$ and $\lambda_{\beta-} = 9.944 \times 10^{-6}\ \mathrm{s}^{-1}$, while for the excited state at 0.04863 MeV, $\lambda_\gamma = 1.439 \times 10^{-10}\ \mathrm{s}^{-1}$ and $\lambda_\alpha = 6.639 \times 10^{-13}\ \mathrm{s}^{-1}$ and for the excited state at 2.3 MeV, $\lambda_{\mathrm{SF}} = 49.5\ \mathrm{s}^{-1}$.

## 1.3 Nuclear Binding Energies and the Semiempirical Mass Formula

### 1.3.1 Nuclear Binding Energies

One of the more important properties of any compound system, whether molecular,

atomic, or nuclear, is the amount of energy needed to pull it apart, or, alternatively, the energy released in assembling it from it constituent parts. In the case of nuclei, these are protons and neutrons. The binding energy of a nucleus ${}^{A}X_{N}$ can be defined as

$$B(A,Z) = ZM_{\mathrm{H}} + NM_{\mathrm{n}} - M_{\mathrm{X}}(Z,A) \quad (1.6)$$

where $M_{\mathrm{H}}$ is the mass of a hydrogen atom, $M_{\mathrm{n}}$ the mass of a neutron, and $M_{\mathrm{X}}(Z,A)$ the mass of a neutral atom of isotope A. Because the binding energy of atomic electrons is very much less than nuclear binding energies, they have been neglected in Eq. (1.6). The usual units are atomic mass units, u. Another quantity that contains essentially the same information as the binding energy is the *mass excess* or the *mass defect*, $\Delta = M(A) - A$. (Another useful quantity is the *packing fraction* $P = [M(A) - A]/A = \Delta/A$.) The most interesting experimental quantity $B(A,Z)/A$ is the binding energy per nucleon, which varies from somewhat more than 1 MeV nucleon$^{-1}$ (1.112 MeV nucleon$^{-1}$) for deuterium (${}^{2}H_{1}$) to a peak near ${}^{56}Fe_{30}$ of 8.790 MeV nucleon$^{-1}$ and then falls slowly until, at ${}^{235}U_{143}$, it is 7.591 MeV nucleon$^{-1}$. Except for the very light nuclei, this quantity is roughly (within about 10%) 8 MeV nucleon$^{-1}$. A strongly bound light nucleus is the α-particle, as for ${}^{4}He_{2}$ the binding energy is 7.074 MeV nucleon$^{-1}$. It is instructive to plot, for a given mass number, the packing fraction as a function of $Z$. These plots are quite accurately parabolas with the most β-stable nuclide at the bottom. The $\beta^-$ emitters will occur on one side of the parabola (the left or lower two side) and the $\beta^+$ emitters on the other side. For odd-$A$ nuclei, there is but one parabola, the β-unstable nuclei proceeding down each side of the parabola until the bottom or most stable nucleus is reached. For the even-$A$ nuclei, there are two parabolas, with the odd–odd one lying above the even–even parabola. The fact that the odd–odd parabola is above the even–even one indicates that a pairing force exists that tends to increase the binding energy of the even–even nuclei. See Figure 1.1 for the $A = 100$ mass chain. Other indications of the importance of this pairing force are the before-mentioned $0^+$ ground states of all even–even nuclei and the fact that only four stable odd–odd nuclei exist: ${}^{2}H_{1}$, ${}^{6}Li_{3}$, ${}^{10}B_{5}$, and ${}^{14}N_{7}$. For even-$A$ nuclei, the β-unstable nuclei zig-zag between the odd–odd parabola and the even–even parabola until arriving at the most β-stable nuclide, usually an even–even one. If the masses for each $A$ are assembled into a three-dimensional plot (with $N$ running along one long axis, $Z$ along a perpendicular axis, and $M(A,Z)$ mutually perpendicular to these two), one finds a ''landscape'' with a deep valley running from one end to the other. This valley is known as the *valley of stability*.

The immediate consequence of the behavior of $B(A,Z)/A$ is that a very large amount of energy per nucleon is to be gained from combining two neutrons and two protons to form a helium nucleus. This process is called *fusion*. The release of energy in the fission process follows from the fact that $B(A,Z)/A$ for uranium is less than for nuclei with more or less half the number of protons. Finally, the fact that the binding energy per nucleon peaks near iron is important to the understanding of those stellar explosions known as *supernovae*. In Figure 1.2, the packing fraction, $P = \Delta/A$, is plotted against $A$ for the most stable nuclei for a given mass number. Note that $P$ has a broad minimum near iron ($A = 56$) and rises slowly until lawrencium ($A = 260$). This shows most clearly the

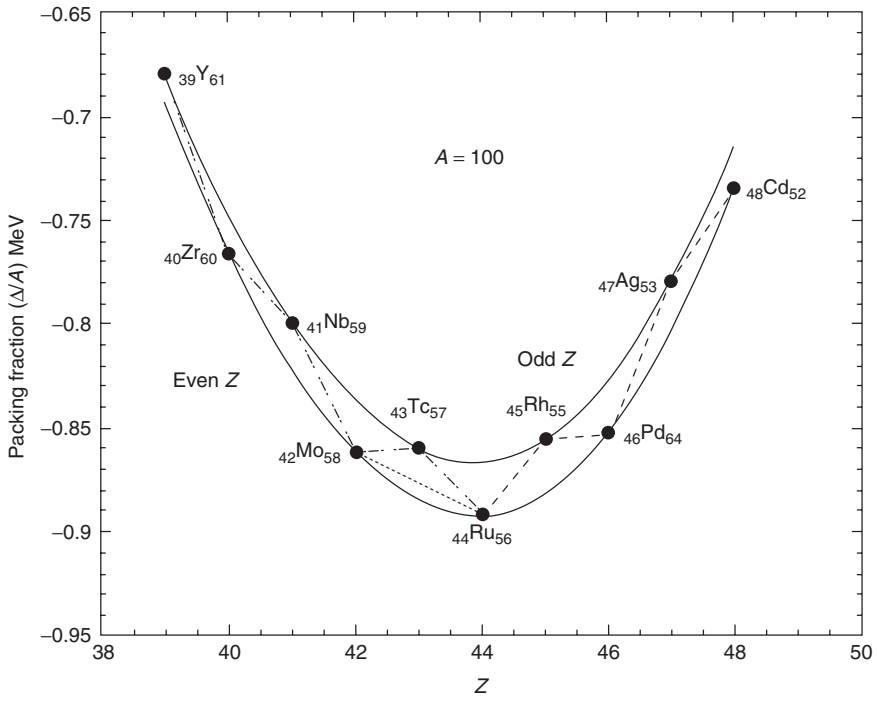


**Figure 1.1** The packing fraction $\Delta/A$ plotted against the nuclear charge $Z$ for nuclei with mass number $A = 100$. Note that the odd–odd nuclei lie above the even–even ones. The $\beta^-$ transitions are indicated by - • -, the $\beta^+$ transitions by ---, while the double β-decay $^{100}_{42}Mo_{58} \rightarrow ^{100}_{44}Ru_{56}$ is denoted by• • •. Data from [14]. The double β-decay from [15].

energy gain from the fission of very heavy elements.

### 1.3.2 The Semiempirical Mass Formula

The semiempirical mass formula may be looked upon as simply the expansion of $B(A,Z)$ in terms of the mass number. Because $B(A,Z)/A$ is nearly constant, the most important term in this expansion must be the term in $A$. From Eq. (1.1) relating the nuclear radius to $A^{1/3}$, we see that a term proportional to $A$ is a volume term. However, this term overbinds the system because it assumes that each nucleon is surrounded by the same number of neighbors. Clearly, this is not true for surface nucleons, and so a surface term proportional to $A^{2/3}$ must be subtracted from the volume term. (One might identify this with the surface tension found in a liquid drop.) Next, the repulsive Coulomb forces between protons must be included. As this force is between pairs of protons, this term will be of the form $Z\{Z-1\}/2$, the number of pairs of $Z$ protons, divided by a characteristic nuclear length or $A^{1/3}$. Two other terms are necessary in this simple model. One term takes into account that, in general, $Z \sim A/2$, clearly true for stable light nuclei, and less so for heavier stable

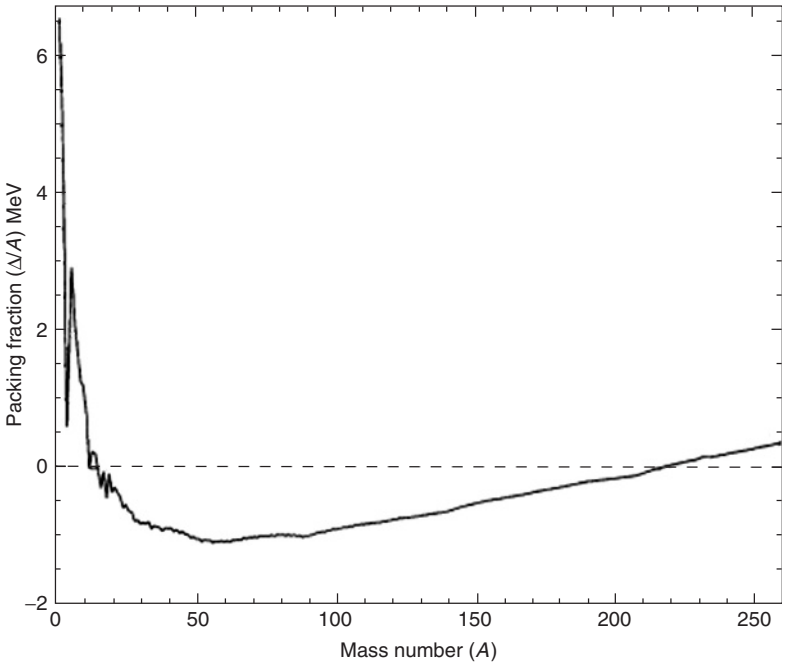


**Figure 1.2** The packing fraction $\Delta/A$ plotted against the mass number $A$ for all nuclei from ${}^{2}_{1}D_{1}$ to ${}^{260}_{103}Lr_{157}$. Data from [14].

nuclei where more neutrons are needed to overcome the mutual repulsion of the protons. This term is generally taken to be of the form $a_{\text{sym}}\ (N-Z)^2/A$. The other term takes into account the fact, noted in Section 1.3.1, that even–even nuclei are more tightly bound than odd–odd nuclei because all of the nucleons of the former are paired off. This is done by adding a term $\delta/2$ that is positive for even–even systems and negative for odd–odd systems and zero for odd-$A$ nuclei. Thus, the two parabolas for even $A$ are separated by $\delta$. From Eq. (1.6), the semiempirical Bethe–Weisäcker mass formula then becomes $M(A,Z) = ZM_{\text{H}} + NM_{\text{n}} - B(A,Z)$ with

$$B(A,Z) = a_{\text{v}}A - a_{\text{s}}A^{2/3} - a_{\text{c}}Z(Z-1)A^{-1/3} - a_{\text{sym}}(N-Z)^2A^{-1} + \frac{\delta}{2} \qquad (1.7)$$

Originally, the constants were fixed by the measured binding energies and adjusted to give appropriate behavior with the mass number [16]. Myers and Swiatecki [17] (see also [18]) have included other terms to account for regions of nuclear deformation, as well as an exponential term of the form $-a_{\text{a}}A\exp(-\gamma A^{1/3})$, for which they provide no physical explanation beyond the fact that it reduces the deviation from experiment. Their model evolved into the macroscopic-microscopic global mass formula, called the *finite-range droplet model* (see [19]) and the *DZ-model* proposed by Duflo and Zuker [20], and more microscopic models, called *HFB* [21]. The many adjustable parameters of the available mass formulas are then fitted to masses of 1760 atomic nuclei [22]. The formulas fit binding energies quite well with errors below 1%, but still

have problems to predict masses far from stability. As those are important for nuclear astrophysics, the measurement of masses of exotic nuclei is an important field today.

A number of consequences flow from even a superficial examination of Eq. (1.7). The fact that the binding energy per nucleon, $B/A$, is essentially constant with $A$ implies that the nuclear density is constant and, thus, the nuclear force saturates. That is, nucleons interact only with a small number of their neighbors. This is a consequence of the very short range of the strong force. If this were not so, then each nucleon would interact with all others in the given nucleus (just as the protons interact with all other protons), and the leading term in $B(A,Z)$ would be proportional to the number of pairs of nucleons, which is $A(A-1)/2$ or roughly $A^2$. This would imply that $B/A$ would go as $A$. Thus, not only does the nuclear force saturate (the Coulomb force does not) but it is also of very short range (that of the Coulomb force is infinite) as the sizes of nuclei are of the order of 3.0 fm (recall Eq. (1.1)).

## 1.4 Nuclear Charge and Mass Distributions

### 1.4.1 General Comments

In his 1911 paper, Rutherford was able to conclude that the positive charge of the atom was concentrated within a sphere of radius $<10^{-14}$ m (10 fm). This result came from α-particle scattering. However, for energetic enough α-particles, the scattering result will contain a component due to nuclear interactions of the α-particle, as well as the Coulomb interaction. For probing the structure of nuclei, electrons have the advantage that their scattering is purely Coulombic; however, to determine details of the internal nuclear structure, electron energies must be well over 100 MeV for their de Broglie wavelengths to be less than nuclear dimensions. Well before the existence of such high-energy electron beams, nuclear structure effects were extracted from information provided by optical hyperfine spectra. In particular, nuclear charge distributions (electric quadrupole moments) and current distributions (magnetic dipole moments) were deduced from very accurate optical measurements (see the following section). A result involving the innermost electrons of heavy atoms is the *isotope shift*, which can be observed in atomic X-rays. This arises because the nuclear radii for two different isotopes of the same atom will produce slightly different binding energies of their K-shell electrons. Thus, the K X-rays of these isotopes will be very slightly different in energy. As an example, the isotopic pair $^{203}\mathrm{T1}_{122}$ and $^{205}\mathrm{T1}_{124}$ have an isotope shift of about 0.05 eV. Another early method to determine the charge radius is to take the difference between the binding energies of two mirror nuclei (cf. Section 1.2.1). This leads to an expression that only involves $a_c$ and, thus, the nuclear radius. This is useful for light nuclei for which mirror pairs occur.

With the advent of copious beams of negative muons, much more accurate optical-type hyperfine spectrum studies could be made. The process is quite simple, and the advantages obvious. By stopping negative muons in a target, an exotic atom is formed in which the muon replaces an orbital electron and transitions to the muonic K-shell follow. These transitions of the muon to the $\mathrm{ls}_{1/2}$ state emit photons of the appropriate (but high) energies. (As the muon is more than 200 times as massive as

the electron, the radii of the muon orbits are reduced by that amount, so that electron-shielding problems are much reduced.) The energies of the photons are such that the $2p_{1/2}-2_{3/2}$ splitting is easily measured (in $^{116}Sn_{66}$, it is 45.666 keV). Thus, both nuclear charge radii and isotope shifts are quite accurately determined. In some recent experiments, root mean square (RMS) charge radii have been measured with a precision of $2 \times 10^{-18}$ m. As electron scattering and muonic atoms are the two methods of measuring characteristics of the nuclear charge radius most susceptible of the greatest accuracy, they will be discussed in turn.

### 1.4.2 Nuclear Charge Distributions from Electron Scattering

In any scattering experiment, what is measured is the differential cross section $(d\sigma/d\Omega)$. Rutherford developed an expression for α-particle scattering that can be used for low-energy, spinless particles incident on a spinless target. Both incident and target particles are assumed to be point particles. The differential cross section for scattering relativistic electrons off point-charged particles leads to the expression for Mott scattering, while, if the target particle has nonzero spin (there is then a magnetic contribution), one obtains the Dirac scattering formula for $(d\sigma/d\Omega)$. However, real nuclei are not point particles, so one needs to make use of the charge form factor $F(\vec{q})$ with $\vec{q}$ the transferred momentum. The form factor $F(\vec{q})$ is then the Fourier transform of the charge density $\rho_{ch}(\vec{r})$:

$$F(\vec{q}) = \int \rho_{ch}(\vec{r}) e^{i\vec{q}\cdot\vec{r}}\, d\tau \qquad (1.8)$$

If one restricts the problem to spherically symmetric distributions, the angular integration of the Fourier integral follows at once, so that

$$F(q) = \frac{4\pi}{q} \int \rho_{ch}(r) \sin(qr) r dr \qquad (1.9)$$

If the target nucleus has zero spin (applicable to all even–even nuclei), then the differential cross sections for a point target and a finite-sized target are related by

$$\frac{d\sigma}{d\Omega} = \left(\frac{d\sigma}{d\Omega}\right)_{\text{Ruth.}} F(q)^2 \qquad (1.10)$$

With the charge form factor determined experimentally, the inverse transform yields the radial charge density

$$\rho_{ch}(r) = \frac{1}{2\pi^2 r} \int F(q) \sin(qr) q dq \qquad (1.11)$$

If the target nucleus is not of spin zero, then an additional term containing the so-called transverse form factor, $F_T(q)$, is needed. (The form factor defined in Eq. (1.9) is sometimes called the *longitudinal form factor*.) In any event, the charge distribution must be normalized to the number of protons ($Z$) in the target nucleus.

At this point, there are two ways to proceed. The first is a model-independent analysis of the form factor, or, second, one can assume a model with several parameters and fit these to the data. Limiting oneself to small momentum transfers, one can obtain the form factor as a power series in $q^2$ by expanding $\sin(qr)$ in Eq. (1.9) in a power series of its argument. Keeping only the lowest term of order $q^2$, one obtains

$$F(q) = Z\left(1 - \frac{1}{6} q^2 \langle r^2 \rangle\right) \qquad (1.12)$$

with

$$\langle r^2 \rangle = \int r^2 \rho_{\mathrm{ch}}(r) 4\pi r^2 \mathrm{d}r \tag{1.13}$$

the RMS radius of the charge distribution. It should be noted that this is not the nuclear radius $R$, which is usually taken as the radius of the constant-density sphere. This yields

$$\langle r^2 \rangle = \frac{3}{5} R^2 \tag{1.14}$$

Data compilations [23] show that for most stable nuclei,

$$R \approx 1.25 A^{1/3} \tag{1.15}$$

As was stated in Section 1.2.1, a better way to describe the charge distribution is to use a Fermi distribution which takes account of the constant charge density, $\rho_0$, at the center of the nucleus and the gradual decrease near the surface. This is achieved by

$$\rho_{\mathrm{ch}}(r) = \rho_0 \frac{1}{1 + \mathrm{e}^{\frac{r - R_{1/2}}{a}}} \tag{1.16}$$

with $R_{1/2}$ the radius at half density and $a$ the diffuseness parameter indicating the distance at which the density falls from 90 to 10% of the constant density $\rho_0$. For heavy nuclei, the following parameterization holds:

$$\begin{aligned} \rho_0 &= 0.17 \frac{Ze}{A}\,\mathrm{fm}^{-3} \\ a &= 2.4\,\mathrm{fm} \\ R_{1/2} &= 1.128 A^{1/3} - 0.89 A^{-1/3}\,\mathrm{fm} \end{aligned} \tag{1.17}$$

There are enough experimental electron-scattering data available throughout all regions of the stable nuclei that quite accurate charge parameters exist for almost all of the systems. The compendium by de Vries *et al*. [23] lists these parameters fitted to the data for several distribution functions in addition to the two-parameter Fermi functions.

### 1.4.3 Nuclear Charge Distributions from Atomic Transitions

During the last decades, tremendous progress was obtained in the study of atomic transitions using high-precision laser spectroscopy. This allows the measurement of nuclear charge radii and also of nuclear moments for stable and even unstable isotopes. This is because the difference between a point nucleus and a finite-size nucleus causes a very small change in the Coulomb potential the atomic electrons feel. A small energy difference on the atomic levels results when we assume that the nucleus is a sphere with constant charge density. For 1s electrons one obtains

$$\Delta E_{1\mathrm{s}} = \frac{2}{5} \frac{Z^4 e^2}{4\pi\varepsilon_0} \frac{R^2}{a_0^3} \tag{1.18}$$

with $a_0$ the Bohr radius. Because no point nucleus exists and the theoretical calculations are not accurate enough to calculate the small shift exactly, one generally measures isotope shifts as the frequency difference of atomic transitions measured in two isotopes of a given element. This then yield the differences in the nuclear radius. Starting from known radii of stable isotopes, it is then possible to determine the radii of unstable nuclei on which one cannot perform electron scattering. It is also possible to measure isotope shifts using optical transitions. Because these are caused by the outermost electrons, the shifts are very small in the order of parts per million. As indicated above, they are still within reach of modern laser techniques.

The small shift for 1s binding energies is related to the large difference between

the Bohr radius and the nuclear radius. On replacing one electron by a muon, the muonic orbits shrink by a factor of 207, the mass difference between the heavy muon and the light electron. At the same time, the muon binding energy is increased by a similar factor, making the transition energies in the mega electron volt region. The energies are so high (in $^{238}U_{146}$, the measured 2p–1s transition is about 6.1 MeV) that one must generate Dirac solutions for the muon moving in a Coulomb potential generated by a non-point-charge distribution. To these initial Dirac solutions, one must add corrections, which, in order of size, are vacuum polarization, nuclear polarization, the Lamb shift, and relativistic recoil. Electronscreening corrections are often included, but they are very tiny (for the ls muonic state in $^{238}U_{146}$, this correction has the value of 11 eV).

As many nuclei are not spherical, several studies have used as the appropriate charge distribution a slightly modified form of Eq. (1.16), which includes the deformations

$$\rho_{\mathrm{ch}}(r) = \rho_0 \left\{ 1 + \exp\left( \frac{r - R_{1/2}\left(1 + \sum_{n=1} \beta_n Y_{n0}(\theta, \phi)\right)}{a} \right) \right\}^{-1} \tag{1.19}$$

Here the $\beta_n$ are deformation parameters that determine the nuclear shape. As an example, the nuclear mean square radius may be expressed as

$$\langle r^2 \rangle_{\mathrm{deformed}} \approx \langle r^2 \rangle_{\mathrm{sph}} \left(1 + \frac{5}{4\pi}\left(\beta_2^2 + \beta_4^2 + \cdots\right)\right) \tag{1.20}$$

Experiments to fit $a$, $c$, and, in deformed regions, $\beta_n$ have been made throughout the periodic table with results consistent with the electron data. However, to combine the results of electron-scattering experiments with those from muonic atoms, it is necessary to use the so-called Barrett moment

$$\left\langle r^k \mathrm{e}^{-\alpha r} \right\rangle = \frac{4\pi}{Z} \int_0^\infty \rho(r) \mathrm{e}^{-\alpha r} r^{k+2} \mathrm{d}r \tag{1.21}$$

where $k$ and $\alpha$ are fitted to the experimental data. The muonic data are equivalent to data from electron-scattering experiments at low momentum transfer. The inclusion of the muonic Barrett moment improves the overall fit by reducing normalization errors. This then reduces the uncertainties over what would be obtained by fitting either the electron-scattering or the muonic atom data alone. Extensive tables of data fitted by various charge distribution models as well as model independent analyzes can be found in de Vries *et al.* [23].

### 1.4.4 Nuclear Mass Distributions

While the measurement of the charge distribution can be made using electromagnetic probes, this is not possible for the mass distribution because of the uncharged neutron. Instead, the nuclear strong force has to be used. This is more

complicated as mostly both Coulomb force and strong force are present. Nevertheless, from α-scattering experiments, information of the mass distribution is obtained. There are also indirect ways in which one can get information on nuclear mass radii. One example is the dependence of α-decay rate on the nuclear radius that defines the Coulomb barrier. In deformed nuclei, this causes an anisotropy because the Coulomb barrier is lower in the direction of the longest axis, making the tunnel probability enhanced. A second way is to use pions instead of muons. These interact with the nucleus through both the Coulomb force and strong force, which, in comparison to muonic atoms, causes an extra shift that allows the determination of the mass radius. The result of these experiments on stable nuclei finds that the charge and mass radii are equal to within about 0.1 fm. This somewhat surprising result can be understood as a balance between the proton Coulomb repulsion that tends to push the protons to the outside and a strongly attractive neutron–proton strong force that tends to pull the extra neutrons to the inward.

Recently, the common opinion that the radii scale with $A^{1/3}$ was found to be heavily violated in more exotic nuclei.

Especially in light nuclei with a large neutron number, so-called halo-nuclei, strong deviations were observed (an early review is given in [24]). Using the radioactive beam techniques, very neutron-rich He, Li, and Be isotopes can be created and studied in the laboratory. It turned out that these loosely bound nuclei show very extended neutron radii whereby two neutrons are moving at radii similar to the radii of Pb isotopes. Moreover, as is the case of $^{11}\mathrm{Li}_8$, the bound system consists of three entities: two neutrons and a $^{9}\mathrm{Li}_6$ that cannot exist two by two, as the dineutron and $^{10}\mathrm{Li}_7$ are unbound. The research on exotic nuclei is still in its infancy and more exotic features such as proton halos or neutron skins are expected. They are of importance as they may influence the creation of the elements under astrophysical conditions.

## 1.5 Electromagnetic Transitions and Static Moments

### 1.5.1 General Comments

Static electromagnetic nuclear moments played an important role in the unscrambling of the detailed measurements of atomic optical hyperfine structure well before the gross components of atomic nuclei were in hand. Almost a decade before the discovery of the neutron, Pauli [7] suggested that the optical hyperfine splitting might be due, in part, to the interaction with a nuclear magnetic moment ($\mu$). This suggestion lay fallow until 1930, when Goudsmit and Young, using the spectroscopic data of Schiller and of Granath, deduced the nuclear magnetic moment of $^{7}$Li to be $\mu = 3.29\mu_{\mathrm{N}}$, where the nuclear magneton equals

$$\mu_{\mathrm{N}} = \frac{e\hbar}{2M_{\mathrm{p}}} = 5.050789 \times 10^{-27}\,\frac{\mathrm{J}}{\mathrm{T}} \tag{1.22}$$

This value is quite close to the currently accepted value ($\mu = 2.327\mu_{\mathrm{N}}$). Because of the existence, by then, of extensive hyperfine optical spectroscopic data, Goudsmit, in 1933, was able to publish a table of some 20 nuclear magnetic moments ranging from $^{7}$Li to $^{209}$Bi. In 1937, Schmidt published a simple, single-particle model of nuclear magnetic moments and supported it with the experimental moments of 32 odd-proton nuclei and 15 odd-neutron

nuclei. This simple model yields what is now known as the *Schmidt limits*, within which almost all nuclear magnetic moments lie (see the following).

The suggestion that the nuclear electric quadrupole moments ($Q$) might also play an important role in optical hyperfine structure was again made before the discovery of the neutron. Racah [8] was the first to work out the theory associated with ''nuclear charge asymmetry'' and the interaction with the atomic electrons. Casimir [25], sometime later, developed the theory of nuclear electric quadrupole hyperfine interaction and applied it to $^{151}$Eu and $^{153}$Eu. In this paper, Casimir mentions work by Schiller and Schmidt, who determined $Q$ for $^{175}$Lu. A short time later, Gollnow [26] obtained $Q = 5.9$ b for this nucleus, quite close to the currently accepted value of 5.68 b. This very large quadrupole moment (very much larger than can be accounted for by the single-particle shell model) was to provide, 20 years later, strong impetus for the development of the collective model of the nucleus. In 1954, Schwartz [27] extended the theory of nuclear hyperfine structure to examine the magnetic octupole hyperfine interaction and calculated the first four nuclear magnetic octupole moments ($O$) from data of the hyperfine structure of the nuclear ground states. The next nuclear moment is the hexadecapole ($H$); however, no direct measurements of such static moments exist. What is known about these moments comes mainly from electromagnetic transitions of electrons and negative muons. For an in-depth theoretical study of all of these moments and how they can be used to test various nuclear models see, in particular, the text by Castel and Towner [28].

Nowadays, the measurement of moments is still very important to assess the single-particle structure of exotic nuclei and several powerful techniques have been developed in this domain [29]. Most information is, however, gathered via the determination of electromagnetic transitions by $\gamma$-ray spectroscopy. This is to a large extent due to the availability of large-volume semiconductor detectors for $\gamma$-ray detection and the high computing power that allows one to analyze more and more complex measured spectra using coincidence conditions. The recent development of $\gamma$-ray tracking detectors out of segmented Ge-detectors offers very high perspectives in the field of exotic nuclei [30].

### 1.5.2 Electromagnetic Transitions and Selection Rules

Without going into a detailed discussion on how matrix elements are calculated, we review here the calculation of electromagnetic transitions. The interested reader can find more details in Heyde [31]. The calculation of transitions and also moments involves the wavefunctions of nuclear states and forms a very sensitive probe for nuclear structure research. On the other hand these transitions and moments are electromagnetic in nature making the interaction very well understood. Using the long-wavelength approximation $\lambda \gg R$ and a multipole expansion of the electromagnetic operators, the transition rates per unit of time can be expressed as

$$T(L) = \frac{2}{\varepsilon_0 \hbar} \frac{L+1}{(L[(2L+1)!!]^2)} \left(\frac{\omega}{c}\right)^{2L+1} B(L) \tag{1.23}$$

with $L$ the multipolarity, $\omega$ the angular frequency of the radiation such that $\hbar\omega \cong E_i - E_f$ up to a small nuclear recoil correction, and $B(L)$ the reduced transition probability

$$B(J_i \to J_f; L) = \sum_{M_i, M_f} \left| \left\langle \alpha_f; J_f M_f \right| O(LM) \left| \alpha_i; J_i M_i \right\rangle \right|^2 \tag{1.24}$$

in units of $e^2 b^L$ and $\mu_N b^{L-2}$ for electric and magnetic $B(LM)$ values. The labels $\alpha$ identify the initial and final states and $O(LM)$ is the electric or magnetic multipole operator of rank $LM$. As all states have good angular momentum, one can now use for the transition rates the Wigner–Eckart theorem to remove all reference to the $M$ projections. This yields

$$B(J_i \to J_f; L) = \frac{1}{2J_i + 1} \left| \left\langle \alpha_f; J_f \| O(L) \| \alpha_i; J_i \right\rangle \right|^2 \tag{1.25}$$

The electric multipole operator for a number of point charges becomes

$$O(E; LM) = \sum_i e_{\text{eff}}(i) r_i{}^L Y_{L,M}(\theta_i, \phi_i) \tag{1.26}$$

with $e_{\text{eff}}(i)$ the effective charge of the $i$th nucleon. Here it is anticipated that owing to core polarization effects and truncations of the model space, other values than the free charges $+e(0)$ for proton (neutron) need to be used. Instead of the operator (Eq. (1.25)), one can also use a similar operator but using the nuclear electric charge density $\rho_{\text{ch}}$ and an integration over the nuclear volume. These are used as several models describe the nucleus as a droplet (Section 1.7). For the magnetic multipole operator, we have

$$O(M; LM) = \sqrt{L(2L+1)} \mu_N \sum_i r_i{}^{L-1} \times \left\{ \frac{e_{\text{eff}}(i)}{e} \frac{2}{L+1} [Y_{L-1} \otimes j_i]^{(L)} + \left( g_s(i) - \frac{e_{\text{eff}}(i)}{e} \frac{1}{L+1} \right) \times \left[ Y_{L-1} \otimes s_i \right]^{(L)} \right\} \tag{1.27}$$

with the effective gyromagnetic ratio $g_s$ which also may differ from the free ones.

The multipole expansion and the fact that states in atomic nuclei have good angular momentum and parity leads to several selection rules. The first one is related to the vector coupling of the angular momentum and states $|J_i - J_f| \le L \le J_i + J_f$. The second is due to the parity of the operators, which clearly is $(-1)^L$ for the electric and $(-1)^{L-1}$ for the magnetic operator. Owing to this, electric and magnetic transitions of order $L$ cannot take place at the same time between states, and moments such as the electric dipole moment are forbidden. While the selection rules allow the determination of the spin and parities of nuclear excited states, they are also (at a higher level) invaluable to test nuclear models (Section 1.7).

Weisskopf has estimated the so-called single-particle values or Weisskopf units (W.u.) by assuming that a single-particle makes a transition with multipole $L$ from a state with spin $L + 1/2$ toward a state with spin $1/2$, that the radial part of the wavefunction can be approximated by a constant value up to the radius $R$, and that certain values for the effective charges hold. This leads to the following estimates for the half-lives corresponding to the single-particle values:

$$T_{1/2}(E1) = \frac{6.764 \times 10^{-6}}{E_\gamma^3 A^{2/3}} \text{ (s)}$$

$$T_{1/2}(M1) = \frac{2.202 \times 10^{-5}}{E_\gamma^3} \text{ (s)}$$

$$T_{1/2}(E2) = \frac{9.527 \times 10^{6}}{E_\gamma^5 A^{4/3}} \text{ (s)}$$

$$T_{1/2}(M2) = \frac{3.102 \times 10^{7}}{E_\gamma^5 A^{2/3}} \text{ (s)}$$

$$T_{1/2}(E3) = \frac{2.045 \times 10^{19}}{E_\gamma^7 A^{2}} \text{ (s)}$$

$$T_{1/2}(M3) = \frac{6.659 \times 10^{19}}{E_\gamma^7 A^{4/3}} \text{ (s)} \quad (1.28)$$

One notices that transition rates of the lower multipolarities are faster than the higher by orders of magnitude and that for a given multipolarity, the electric ones are about 100–1000 faster as the magnetic ones. Owing to the selection rules and enhanced quadrupole collectivity, only $E2$ and $M1$ transitions happen on similar timescales. In this case, one has a transition of mixed multipolarity.

The Weisskopf estimates are very crucial to determine whether a transition is caused by a single nucleon changing orbits or by several nucleons acting in a collective way. The measurement of transition rates of excited states delivers very important information on nuclear structure, but is also quite involved. One needs to measure the lifetime of a state, the (mixed) multipolarity, and the energy and intensities of the transitions deexiting a given state. To this end, $\gamma$-ray arrays consisting of several Ge-detectors are appropriate. Besides this, electromagnetic decay can also take place with the emission of conversion electrons. These electrons allow one to determine the multipolarity as well as to observe the by $\gamma$-emission forbidden $E0$ transitions (due to the fact that the photon has spin 1 with projection +1 and −1).

### 1.5.3 Static Moments

In contrast to the transition rates, the *multipole moments* are generally defined as the matrix element of the $M = 0$ component of the moment operator for a single state with magnetic projection $M = +J$. Of the moments, the two lowest are the most important.

#### 1.5.3.1 Magnetic Dipole Moments

If one assumes that the magnetic properties are associated with the individual nucleons, then the magnetic moment is defined as

$$\mu = \langle \alpha, JJ | \sum_i g_l(i) l_{z,i} + g_s(i) s_{z,i} | \alpha; JJ \rangle \quad (1.29)$$

where the sum extends over all of the $A$ nucleons. Generally, this will not be needed; for instance, the magnetic moment of an odd-$A$ nucleus will be generated by the last neutron and proton as the adjacent even–even ground state has no magnetic moment. In Eq. (1.29), $g_l$ and $g_s$ are the orbital and spin gyromagnetic ratios. They are often chosen as $0.7 g_{\text{free}}$ where the free-particle values are $g_l = 1$, $g_s = 5.587$ for protons and $g_l = 0$, $g_s = -3.826$ for neutrons (all in $\mu_N$). It is instructive to calculate the magnetic moment for a single nucleon (which, as explained earlier, is a good approximation for the ground state of odd-$A$ nuclei). Using the total angular momentum and the Wigner–Eckart theorem, one deduces the single-particle magnetic moments for aligned and antialigned orbital momentum and spin:

$$\mu(j = l + 1/2) = j \left( g_l + \frac{(g_s - g_l)}{2} \right) \quad (1.30a)$$

$$\mu(j = l - 1/2) = \left( j g_l - \frac{j}{j+1} \frac{(g_s - g_l)}{2} \right) \quad (1.30b)$$

The magnetic moments plotted as a function of spin form the so-called Schmidt lines. It is interesting that, when plotted, almost all of these moments lie between the Schmidt lines. The moments that

lie outside these limits occur mainly for some very light nuclei. One may conclude that the single-particle model does possess some validity. Another set of limits, the Margenau–Wigner (M-W) limits, is obtained by replacing the free-particle values for the orbital gyromagnetic ratios, $g_l$, by the uniform value $Z/A$. The justification for this is that one is in effect averaging over all states that lead to the correct nuclear spin. This calculation represents an early attempt to account for core contributions to the dipole-moment operator. Figure 1.3 and Figure 1.4 show plots of a number of the ground-state magnetic moments for odd-$Z$ (Figure 1.3) and odd-$N$ (Figure 1.4) nuclei.

Besides the ground state, excited states can have magnetic moment and their measurement is often used to extract information on the underlying single-particle structure. Common in nuclear structure physics is the use of $g$-factors that are analogous to the single-particle gyromagnetic ratios, except that they are dimensionless. They are defined as

$$\mu = gI\mu_N \tag{1.31}$$

One way to determine the $g$-factor is to measure the Lamor frequency when excited nuclei are placed in an external magnetic field $B$. Then,

$$\omega_L = \frac{gB\mu_N}{\hbar} \tag{1.32}$$

The main problem hereby is to align the spins of an ensemble of atomic nuclei.

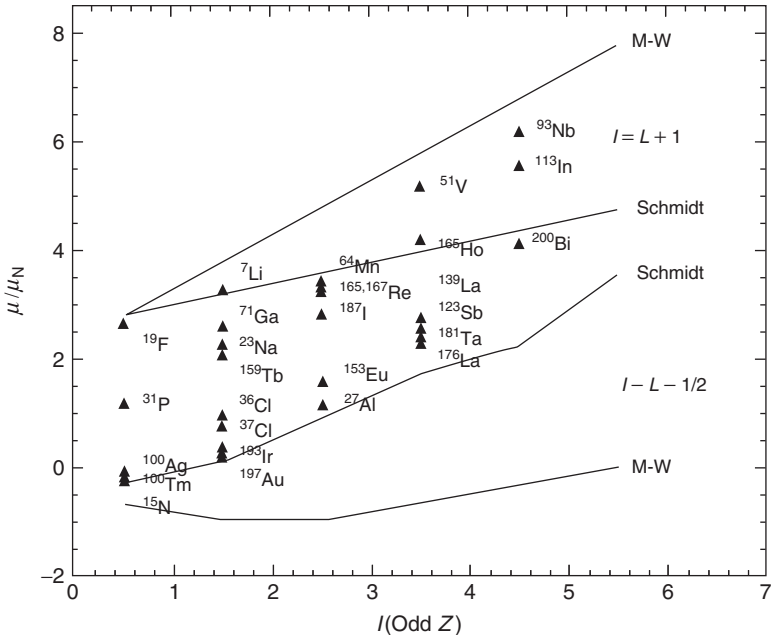


**Figure 1.3** Nuclear magnetic moments in units of the nuclear magneton ($\mu/\mu_N$) plotted against the nuclear spin ($I$) for a number of odd-$Z$ nuclei. The Schmidt limits, as well as the Margenau–Wigner (M-W) limits, are shown as solid lines. Data from [14].

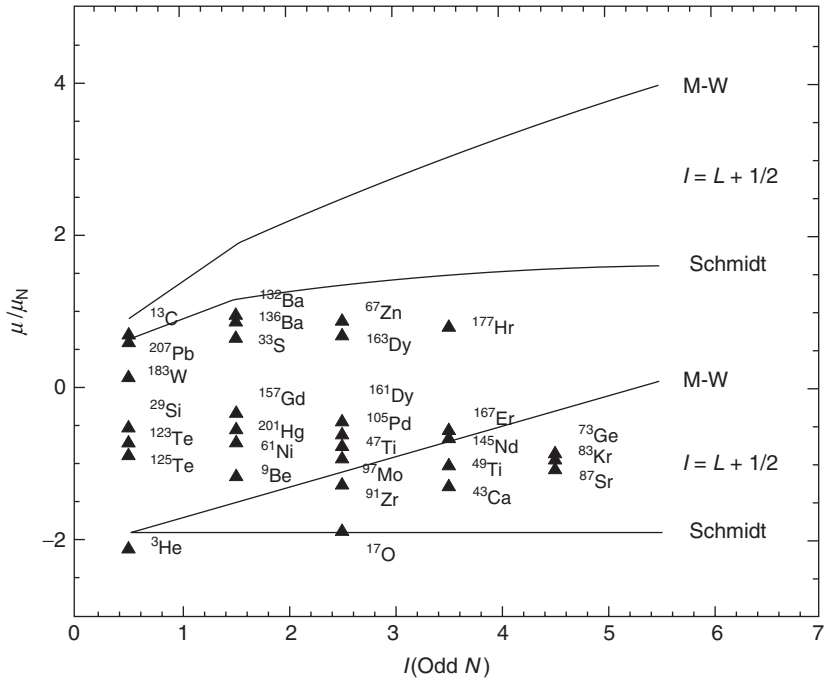


**Figure 1.4** Nuclear magnetic moments in units of the nuclear magneton ($\mu/\mu_N$) plotted against the nuclear spin ($I$) for a number of odd-$N$ nuclei. The Schmidt limits, as well as the Margenau–Wigner (M-W) limits, are shown as solid lines. Data from [14].

This has to be done by the nuclear reaction used, cooling in an external magnetic field, or via the observation of changes in angular correlations.

#### 1.5.3.2 Electric Quadrupole Moments

As a general definition of the quadrupole moment, we have the expectation value of $(3z^2 - r^2)$. Using the proportionality of the quantity with $Y_{20}(\theta,\phi)$ one gets

$$Q(J) = \sqrt{\frac{16\pi}{5}} \times \left\langle \alpha; JJ \left| \sum_i \frac{e_{\text{eff}}(i)}{e} r_i^2 Y_{2,0}(\theta_i, \phi_i) \right| \alpha; JJ \right\rangle \tag{1.33}$$

or, using the Wigner–Eckart theorem,

$$Q(J) = \sqrt{\frac{16\pi}{5}} \sqrt{\frac{J(2J-1)}{(2J+1)(2J+3)(J+1)}} \times \left\langle \alpha; J \left\| \sum_i \frac{e_{\text{eff}}(i)}{e} r_i^2 Y_2(\theta_i, \phi_i) \right\| \alpha; J \right\rangle \tag{1.34}$$

The quadrupole moment can also be calculated for a single nucleon in an orbit $j = J$. This yields

$$Q(j) = -\frac{(2j-1)}{(2j+2)} \frac{e_{\text{eff}}(i)}{e} \langle r^2 \rangle \tag{1.35}$$

One thus obtains a negative quadrupole moment for a single nucleon. If the orbit

is filled up to a single hole, a quadrupole moment as in Eq. (1.35) but with a positive sign is expected. We would like to illustrate the application of Eq. (1.35) with examples near the doubly magic nucleus $^{16}O_8$ (see also Section 1.7). The orbit that the ninth nucleon can occupy has $j = 5/2$ and we can use Eqs. (1.13) and (1.14) to estimate $<r^2>$. This yields for $^{17}F_8$ using the free-proton charge $Q = -5.9\,\mathrm{fm}^2$, which is in excellent agreement with the experimental absolute value given in Firestone *et al.* (1996) of $|Q| = 5.8(4)\,\mathrm{fm}^2$. For the odd neutron nucleus $^{17}O_9$, one finds experimentally $Q = -2.578\,\mathrm{fm}^2$, which shows the need for effective charges and can be reproduced using $0.44e$ as neutron effective charge. Finally, if we place five neutrons in the $j = 5/2$ orbit, we have the $N = 13$ isotones and expect moments of $Q = +2.6\,\mathrm{fm}^2$. Experimentally, one finds $Q = 20.1(3)\,\mathrm{fm}^2$ in $^{25}Mg_{13}$ and $Q = 10.1(2)\,\mathrm{fm}^2$ in $^{23}Ne_{13}$. This observation of much larger quadrupole moments occurs for most atomic nuclei having several nucleons in an orbit or in several orbits, indicating that the model is too simple and that all of the electric charges must be considered. This holds especially if the core is not spherically symmetric and the motion becomes collective.

## 1.6 Excited States and Level Structures

### 1.6.1 The First Excited State in Even–Even Nuclei

The most obvious characteristic of the various nuclei is that all of the even–even nuclei have ground-state spins and parities of $0^+$. This not only categorizes one large group of nuclei but also indicates that the nuclear force is such that it couples, preferentially, pairs of like nucleons to angular momentum zero. The second observation is that the first excited state in even–even nuclei is almost always a $2^+$ excitation. This can be understood by the combination of good total angular momentum and the Pauli principle. If one couples two nucleons in orbit $j$ and implies the antisymmetrization, one obtains

$$\varphi(j,j;JM) = \frac{1}{2}\sum_{mm'}(jmjm'|JM)(\psi_1(jm)\,\psi_2(jm') - \psi_2(jm)\psi_1(jm')) \tag{1.36}$$

with the Clebsch–Gordan coupling coefficient for the angular momentum coupling. This can, however, be rewritten as the $m$-values are in the summation. Using the symmetry properties, one arrives at

$$\varphi\,(j,j;JM) = \frac{1}{2}\left(1-(-1)^{2j-J}\right) \times \sum_{mm'}(jmjm'|JM)\,\psi_1(jm)\psi_2(jm') \tag{1.37}$$

The phase factor, and the fact that $2j$ is an odd number, imply that states with odd values of $J$ do not exist. One might wonder whether this is an essential property of fermions, but surprisingly it is not. Consider bosons with integer angular momentum $\ell$. Then, owing to symmetrization, Eq. (1.36) becomes

$$\varphi(\ell,\ell;JM) = \frac{1}{2}\sum_{mm'}(\ell m\ell m'|JM) \times(\psi_1(\ell m)\psi_2(\ell m') + \psi_2(\ell m)\psi_1(\ell m')) \tag{1.38}$$

which yields after reordering,

$$\varphi(\ell,\ell;JM) = \frac{1}{2}\left(1+(-1)^{2\ell-J}\right)\sum_{mm'} \times(\ell m\ell m'|JM)\psi_1(\ell m)\psi_2(\ell m') \tag{1.39}$$

but now $2\ell$ is even and again all states with odd $J$-values disappear. The fact that both bosons and fermions yield similar results is very important for nuclear models. It means that one can often describe even–even atomic nuclei using either fermionic nucleons or collective bosons such as phonons.

### 1.6.2 Regions of Different Level Structures

The existence of a low-lying $2^+$ excitation can be explained in different ways, that is, short-range interaction, a collective quadrupole vibration, or as a first excited state of a rotational band. Which interpretation is right or better and which mixture of interpretations is right depends a lot on where on the Segre chart the nucleus is located and how the higher excitations behave. This is illustrated in Figure 1.5, which shows the known energies of the first excited states in the even–even Cd and Hf isotopes. One notices huge differences in the absolute excitation energies but also a quite smooth behavior. If one now also considers the next excited state, which is a $4^+$ excitation and plots the ratio $R4/2$,

$$R4/2 = \frac{E_{\mathrm{exc}}(4^+)}{E_{\mathrm{exc}}(2^+)} \tag{1.40}$$

(see also Figure 1.5) more information can be obtained. In the Hf isotopes, a clear saturation near $R4/2 = 3.33$ occurs indicating that a rotational band, with its typical $I(I+1)$ energy dependence, is built on the ground state. For Cd, we observe very high $2^+$ excitation energies and low $R4/2$ ratios at the beginning and end of the isotope chain. This is a clear evidence that at the extremes, a shell closure occurs, when $N = 50$ and 82. In the middle, one finds, compared to Hf, much higher $2^+$ excitation energies and $R4/2$ ratios slightly above 2, indicating an anharmonic quadrupole vibrational nature at mid shell.

While the strong pairing of like nucleons can explain the ground state of even–even nuclei, it does not yield predictions for the ground-state spins and parities of odd-$A$ and odd–odd nuclei. Nevertheless, it simplifies this task a lot, as in most cases one can conclude that the ground-state spin and parity of an odd-$A$ nucleus is equal to the one of the last odd nucleon. This forms an important testing ground for the shell model, which predicts the single-particle energy, spin, and parity of the subsequent orbits.

### 1.6.3 Shell Structures

Various sets of nuclear data indicate that certain numbers of nucleons, either neutrons or protons, correspond to the filling of angular momentum "shells." These are similar to the atomic shells often denoted as the K-shell, L-shell, and so on. In nuclei, the shell filling is similar but not identical, and the principal shell closings occur at experimentally observed numbers. These are for either *N or Z* equal to 2, 8, 20, 28, 50, 82, and 126. These are the *magic numbers*. They occur where there are drastic changes in neutron cross sections, nucleon separation energies, and so on. An interesting, but small, group of nuclei comprises the doubly magic ones – that is, nuclei with both neutron and proton numbers magic. The five stable ones are $^4\mathrm{He}_2$, $^{16}\mathrm{O}_8$, $^{40}\mathrm{Ca}_{20}$, $^{48}\mathrm{Ca}_{28}$, and $^{208}\mathrm{Pb}_{126}$. Note that no stable doubly magic nuclei with 50 and 82 exist. What is notable about the doubly magic nuclei is that their first excited states are at a very

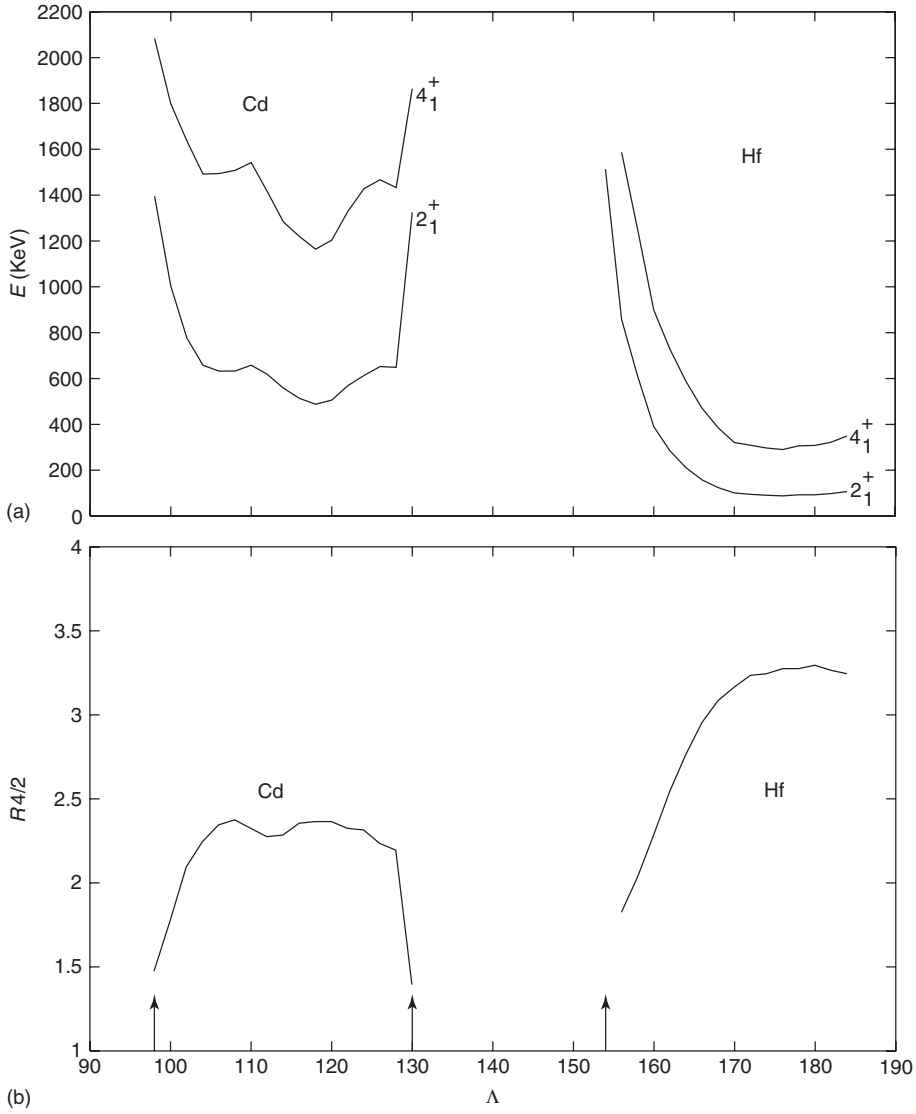


**Figure 1.5** The known energies of the first excited states in the even–even Cd and Hf isotopes (a). The $R4/2$ ratios are also given (b). The left side represents the Cd isotopes and the right side the Hf isotopes. Arrows mark the closed shells at $A = 98$, 130, and 154.

high energy compared with their non-doubly magic neighbors. The energy in megaelectronvolts, spin, and parity of these first excited states is 20.1, $0^+$; 6.05, $0^+$; 3.35, $0^+$; 3.83, $2^+$; and 2.61, $3^-$, respectively. Also the observed spins (and parities) of the first excited states is very different from that of all other even–even nuclei.

Because of these large gaps or changes in nuclear properties, they divide the low-lying excited states of nuclei into roughly three regions. These are, broadly, the nuclei in the neighborhood of the magic numbers that are dominated by shell or single-particle structures and those further away, which show collective behavior. Of particular interest are the ones found between these two, as they may give clues to the onset of collective motion in atomic nuclei and other systems. We mentioned earlier that 126 is a magic number, but strictly speaking, this holds only for neutrons as the unstable element with $Z = 126$ has not yet been observed. Nowadays, there is a strong interest to study whether magic numbers still stay valid in exotic nuclei far from stability and which is the next magic number for superheavy isotopes.

### 1.6.4 Collective Structures

Within major divisions (even–even, odd-$A$, and odd–odd), the excited levels are further divided into groups that are single-particle or collective (vibrational or rotational) in nature. However, because of the strong pairing force, even–even nuclei do not show single-particle excited levels but rather one- or two-particle-hole excitations or two-quasiparticle excitations. Here, we introduce the most general features of the two major classes of collective nuclei. We restrict ourselves to even–even nuclei for the sake of simplicity.

#### 1.6.4.1 Vibrational Levels

The intermediate systems between the tightly bound magic nuclei and the deformed nuclei are the so-called vibrational nuclei. Here the number of nucleons outside of a deformable core is small, and the zero-point energy of the lowest oscillations is greater than the energy of deformation, so that the shape of the core is not stabilized. The motion then is of quantized surface oscillations with angular momentum two. One can introduce creation and destruction phonon operators $Q^+_{LM}$ and $Q_{LM}$ which fulfill the boson commutation rules:

$$[Q_{LM}, Q^+_{LM}] = \delta_{LL'}\delta_{MM'} \tag{1.41}$$

and for which all other commutators are zero. The angular momentum of the phonon is $L$, its magnetic projection $M$ and its parity $\pi = (-1)^L$. The magnetic projection is mostly not of great importance. In this representation, the number operator counting the number of $L$ phonons is given by

$$\widehat{N}_L = \sum_M Q^+_{LM} Q_{LM} \tag{1.42}$$

Using the number operator, the simplest Hamiltonian becomes

$$\widehat{H} = \sum_L \hbar\omega_L \left(\widehat{N}_L + L + \frac{1}{2}\right) \tag{1.43}$$

where the additional factors are chosen such that the Hamiltonian corresponds to the quantized harmonic oscillators for $L$ phonons. Each of the phonons has energy $\hbar\omega_L$. Because most even–even nuclei have as first excited state a $2^+$ state, the $L = 2$ quadrupole phonons are dominant. At higher energy, there is evidence for the presence of $L = 3$ octupole phonon making a $3^-$ state. Using the energy solution of the Hamiltonian equation (Eq. (1.43)),

$$E(N_L, L) = \sum_L \hbar\omega_L \left(N_L + L + \frac{1}{2}\right) \tag{1.44}$$

and the proper angular momentum coupling and symmetrization given in Eq. (1.39), one arrives at a very simple prediction. The one-quadrupole phonon state has $L=2$ and $E_{\rm exc}=\hbar\omega_2$ and the two-phonon states have $L=0$, 2, 4 and $E_{\rm exc}=2\hbar\omega_2$. This exactly yields the $R4/2$ ratio of 2 observed in Figure 1.5.

A nice example of a "good" vibrational even–even nucleus is $^{110}Cd_{62}$. The first excited $2^+$ state is at 0.6578 MeV followed by a $0^+$, $2^+$, $4^+$ states at 1.473, 1.476, and 1.542 MeV. The ratio $R4/2=2.35$ is somewhat larger than the one the simple model gives.

#### 1.6.4.2 Rotational Levels

If the number of nucleons outside the deformable core is such that the zero-point oscillations are much less than the energy of deformation, then the system will have a stable but deformed shape and one must quantize a rigid rotator. From classical considerations, we know that, if the system has a permanent, nonspherical shape, there exists a body-fixed system in which the inertial tensor $\mathfrak{I}$ is diagonal and is related to the laboratory-fixed system by an Euler transformation. We denote these two coordinate systems as (1,2,3) and ($x$,$y$,$z$), respectively. The inertial tensor then has components $\mathfrak{I}_1$, $\mathfrak{I}_2$, and $\mathfrak{I}_3$, so that the Hamiltonian is just

$$\widehat{H}=\frac{1}{2}\left(\frac{\widehat{L}_1^2}{\mathfrak{I}_1}+\frac{\widehat{L}_2^2}{\mathfrak{I}_2}+\frac{\widehat{L}_3^2}{\mathfrak{I}_3}\right) \tag{1.45}$$

with $\widehat{L}_{1,2,3}$ the body-fixed angular momentum. The simplest system is the one for which all moments of inertia are equal: $\mathfrak{I}_1=\mathfrak{I}_2=\mathfrak{I}_3=\mathfrak{I}$. Then the energies are directly found:

$$\widehat{H}=\frac{\hbar^2}{2\mathfrak{I}}(L(L+1)) \tag{1.46}$$

The system specified by Eq. (1.45) possesses the symmetry properties belonging to the point group $D_2$ for which four representations exist. The Hamiltonian operator (Eq. (1.45)) does not mix different representations. The basis functions are those of a symmetric top, $|LMK>$ being diagonal in $\boldsymbol{L}^2$, $\boldsymbol{L}_z$, and $\boldsymbol{L}_3$ with the usual eigenvalues $L(L+1)$, $M$, and $K$, respectively. Here $K$ is the projection of the angular momentum on the body-fixed frame. Applying this formula for the ground-state rotational band with $K=0$, we find now $R4/2=3.33$. However, states with different $K$-values are degenerated. This is not found in real deformed nuclei.

If the inertia tensor is such that $\mathfrak{I}_1\neq\mathfrak{I}_2\neq\mathfrak{I}_3$, an asymmetric top problem results. In this case, the wave functions are to be expanded in terms of the symmetric-top functions:

$$|LM\rangle=\sum_{K=-L}^{+L}A_K\,|LMK\rangle \tag{1.47}$$

The 1, 2, 3 labels of the momental ellipsoid's semiaxes are quite arbitrary and can be chosen in 24 different ways for right- (left-) handed systems. These 24 relabelings can be produced by three different relabeling transformations $T_1$, $T_2$, and $T_3$ [32], which correspond to label interchanges and operate on the $|LM>$ wave functions. They have the properties

$$T_1^2=T_2^4=T_3^3=1 \tag{1.48}$$

From these relations, one can generate Table 1.1, relating the four representations and the values of angular momentum and parity allowed in each. Note in particular that the $A$ and $B_2$ representations are associated with positive-parity ($\pi=+$) states, while $B_1$ and $B_3$ representations are associated with negative parity ($\pi=-$)

**Table 1.1** The representation of the point group $D_2$ to which the states belong, and the allowed values of the angular momentum and parity associated with them.

| Representation | $K$ | Parity | Allowed $L$-values |
|---|---|---|---|
| $A$ | Even | + | $L = 0,2,2,3,4,4,4,5,5$ |
| $B_1$ | Even | − | $L = 1,2,3,3,4,4,5,5,5$ |
| $B_2$ | Odd | + | $L = 1,2,3,3,4,4,5,5,5$ |
| $B_3$ | Odd | − | $L = 1,2,3,3,4,4,5,5,5$ |

states. From this table, we note that only the rigid rotator systems belonging to the $A$ representation have a zero angular momentum state. They must be associated with the lowest levels of even–even nuclei and form the $K = 0$ ground-state band with $K = 0$ and $L = 0, 2, 4, 6, \ldots$ followed by the $\gamma$-vibrational band with $K = 2$ and $L = 2, 3, 4, 5, \ldots$.

Negative-parity states in even–even nuclei could be associated with either the $B_1$ or $B_3$ representations. If one argues that, given two (or more) possibilities, the lowest set of states will be the most symmetric, then because the $B_1$ representation arises from sums over even $K$ quantum numbers, one should associate this representation with the lowest-lying negative-parity states in even–even systems. Furthermore, in the deformed regions, the negative-parity bands in these nuclei not only lie above the ground-state rotational band but they also have as their band head a $1^-$ level. This is another indication that these negative-parity rotational bands belong to the $B_1$ representation.

The problem of solving the asymmetric, rigid rotor is far more involved than the symmetric rotor as all of the latter's eigenvalues can be given in closed form. To proceed along this line, one sets $\mathfrak{I}_0 = \mathfrak{I}_1 = \mathfrak{I}_2 \neq \mathfrak{I}_3$. The Hamiltonian of the system then becomes

$$\begin{aligned}\widehat{H}_{\text{sym}} &= \frac{1}{2}\left(\frac{\widehat{L}_1^2 + \widehat{L}_2^2}{\mathfrak{I}_0} + \frac{\widehat{L}_3^2}{\mathfrak{I}_3}\right) \\ &= \frac{1}{2}\left(\frac{\widehat{L}^2}{\mathfrak{I}_0} + \left(\frac{1}{\mathfrak{I}_3} - \frac{1}{\mathfrak{I}_0}\right)\widehat{L}_3^2\right) \quad (1.49)\end{aligned}$$

and both of the operators appearing are diagonal. Thus, we obtain immediately the eigenvalues

$$E_{\text{sym}} = \frac{h^2}{2}\left(\frac{L(L+1)}{\mathfrak{I}_0} + \left(\frac{1}{\mathfrak{I}_3} - \frac{1}{\mathfrak{I}_0}\right)K^2\right) \quad (1.50)$$

This expression is model independent and only depends upon the ratio of the moments of inertia $\mathfrak{I}_0/\mathfrak{I}_3$. There have been recent observations of "superdeformation" for rare earth nuclei with spheroidal-axes ratios of 2 : 1. For symmetric rotational systems with $K = 0$, the ratio $R4/2$ is 10/3 rather than 2 for the vibrational systems. Thus, this ratio differentiates well between rotational and vibrational systems. In recent years, there was quite some interest in how these shape changes occur [33, 34], as they can be treated as quantum-phase transitions. Atomic nuclei that have an $R4/2$ ratio of around 2.9 lie at the critical point of the spherical-deformed phase transition.

## 1.6.5 Odd-A Nuclei

### 1.6.5.1 Single-Particle Levels

Near the magic numbers, the ground and lower excited states appear to be mainly single-particle states, that is, states that do not seem to possess collective properties. For instance, near the doubly magic nucleus $^{16}O_8$, one finds that both $^{15}N_8$ and $^{15}O_7$ have $1/2^-$ ground states and nearly identical lower excited states. This shows that the $N = Z = 8$ shell is filled by a $p_{1/2}$ orbit. Above the closed shell are $^{17}F_8$ and $^{17}O_9$ both of which have the expected $5/2^+$ ground state from the $d_{5/2}$ orbit. These data clearly support the notion that angular momentum shells are filled in a manner similar to the electronic shells of the elements.

### 1.6.5.2 Vibrational Levels

The nucleons all possess intrinsic spin 1/2 and angular momentum $l$, so that the simplest model for vibrational odd-$A$ nuclei that one might construct is to add a single nucleon to an even–even core in which the nucleons of each kind pair to zero angular momentum. If the core is a good vibrational nucleus ($R4/2 \sim 2$), then the ground state of the odd-$A$ system will have the angular momentum properties of the odd nucleon. Furthermore, by coupling this nucleon to the excited states of the core, one should expect to be able to determine the angular momenta of the odd-$A$ nucleus's excited states. An example is the coupling of a neutron to the vibrational nucleus $^{110}Cd_{62}$ (Section 1.6.2) to yield the odd-$A$ nucleus $^{111}Cd_{63}$, which has a ground-state spin of $1/2^+$. One might expect that there would be two excited states built on the first excited $2^+$ state with spins $3/2^+$ and $5/2^+$. This nucleus does indeed have a $3/2^+$, $5/2^+$ pair as its first excited states, which are at 245.4 and 342.1 keV. Coupling of the $1/2^+$ neutron with the two-phonon states would lead to excited state spins from $1/2^+$ through $9/2^+$. Such a set of states does appear at higher energies. However, it is difficult to pick out which states might belong to the two-phonon core states. Below them there is a first negative parity state with spin $11/2^-$ at 396.22 keV, which indicates that one has the presence of a low-lying $h_{11/2}$ neutron orbit.

### 1.6.5.3 Rotational Levels

One might expect that a simple model for the odd-$A$ rotational levels would follow that of the vibrational levels. However, the experimental data do not show such a similar structure. As an example we consider $^{157}Gd_{93}$ which has a $3/2^-$ ground state. Following the reasoning for vibrational nuclei, one expects from the coupling with the first excited 2+ state a multiplet with spins $1/2^-$, $3/2^-$, $5/2^-$, and $7/2^-$. Instead, one observes a rotational-like band with the spin sequence: $5/2^-$, $7/2^-$, $9/2^-$, $11/2^-$, .... This is due to the fact that the ground-state band has also a given value of $K$ and we conclude that $K = 3/2$.

## 1.6.6 Odd–Odd Nuclei

As noted in Section 1.6.1, there are only four stable odd–odd nuclei; however, a great deal of data exist for all of this class of nuclei. Again, one might feel that these nuclei would be well represented by an even–even core plus a neutron–proton pair. Even if these are coupled to a spin-zero core, there is still considerable ambiguity as to how these couple to form the ground-state spin of the system. For instance, if the proton and neutron angular momenta are $j_p$, $j_n$, respectively, then their vector sum

can lead to the range of $J$ values

$$\left|j_p - j_n\right| \leq J \leq j_p + j_n \tag{1.51}$$

One can obtain the values of $j_p$ and $j_n$ from the ground-state spins of the neighboring odd-$A$ nuclei with one less neutron or one less proton, respectively. In order to determine more exactly the range of the possible ground-state spins of these nuclei, one must make use of Nordheim's rules, which are the following:Strong rule, for $\eta = 0$:

$$J = \left|j_p - j_n\right| \tag{1.52}$$

Weak rule, for $\eta = \pm 1$:

$$J = \left|j_p - j_n\right| \text{ or } j_p + j_n \tag{1.53}$$

with

$$\eta = (j_p - l_p) + (j_n - l_n) \tag{1.54}$$

In general, these do not work all of the time. To predict the excited states spins is even more difficult, making odd–odd nuclei the most difficult to describe.

## 1.7 Nuclear Models

### 1.7.1 Introduction

The nucleus, being a many-body collection of $A$ particles interacting through a short range but strong force, is not easily dealt with. From a theoretical point of view, making use of an accurate many-body calculation is impossible because these are beyond the scope of current theoretical methods. Thus, calculations based upon various simple models are able to provide a good deal of physical insight as well as making predictions of measurable properties, providing a way to categorize the vast amounts of data available from nuclear physics laboratories. While these approaches may seem to be organized in an historical order, all are to greater or less extent being continuously refined.

The nuclear many-body problem is not solved definitely, owing to the large number of strongly interacting particles. To illustrate the difficulties, we take the example of $^{208}$Pb. If we consider up to two-body interactions between the nucleons, the general Hamiltonian is given by

$$H = \sum_{i=1}^{208} t_i + \frac{1}{2}\sum_{i \neq j}^{208} V_{ij} \tag{1.55}$$

The radius of this nucleus is 7 fm, while the strong force between two nucleons varies significantly on the scale of 0.2 fm. If one would calculate only the two-body interaction on a mesh, one should foresee for each nucleon at least 100 mesh points in each direction and for all 208 nucleons the number of possible combinations would be $100^{3.208}$. For a fast computer today $10^9$ operations per second are feasible, which gives $10^{16}$ operations per year. Thus to perform the calculation one would need $10^{1232}$ years, while the age of our universe is only $2 \times 10^{10}$ years.

As an exact treatment is impossible, one of the major characteristics of nuclear structure calculations is the choice of the right approximations and truncations needed to make a calculation feasible while keeping the essential physics. Of great help thereby is the extensive use of symmetry concepts, which allow one to simplify the many-body problem and make the calculations tractable. Many quite different approaches have turned out to be

successful for certain classes of atomic nuclei. Most theoretical models rely on spherical symmetry, which allow the use of the very powerful "Racah machinery," originally developed for atomic physics by Guilio Racah. The introduction of irreducible tensors and coupling coefficients then provides the necessary technical skills to perform nuclear structure calculations.

The first approach is based on the experimental observation of magic numbers and leads to the nuclear shell model as described in Section 1.7.2. In Section 1.7.3 we introduce the deformed shell model, which allows the description of medium-heavy nuclei that are deformed. Section 1.7.4 is devoted to the collective model in which medium heavy and heavy nuclei are described by a quantum liquid droplet.

In Section 1.7.5, we will deal with a new theoretical approach to many-body problems originating from nuclear physics: the interacting boson approximation (IBA). Although the IBA is a method that was developed to describe the atomic nucleus, it has since been applied to molecules, quarks, and fullerenes. The major assumption of the interacting boson model (IBM) is twofold. First, because of the shell structure evinced by many experiments, only the valence nucleons are considered to be important for the low-energy excited states of the atomic nucleus. Those move to a first approximation in orbits formed by their commonly created average field, which is spherical symmetric. Secondly, between like nucleons, either protons or neutrons, there is a dominant pairing force when they occupy the same orbit. This allows to replace coupled fermion pairs by real bosons that are simpler to deal with.

### 1.7.2 The Spherical-Shell Model

One of the first and best understood nuclear models is the nuclear shell model. The major assumption of this model is that nucleons up to a good approximation move independently in a spherically symmetric averaged field $U(r_i)$ created by the other nucleons. This means that the many-body Hamiltonian is rewritten as

$$H = H_0 + V_{\text{res}} \tag{1.56}$$

with

$$H_0 = \sum_{i=1}^{N} t_i + \sum_{i=1}^{N} U(r_i) \tag{1.57}$$

and the residual interaction $V_{\text{res}}$ is given by

$$V_{\text{res}} = \frac{1}{2}\sum_{i\neq j}^{N} V_{ij} - \sum_{i=1}^{N} U(r_i) \tag{1.58}$$

The shell model uses the ansatz (Eq. (1.57)) in which the single particles move in a potential well provided by the other particles. While it might seem improbable that nuclei made up of a large number of strongly interacting particles could in any way be represented by such a model, one must recall that the Pauli principle prevents most interactions of a nucleon in the nucleus. In general, scattering cannot take place, as most of the states into which a low-energy nucleon can scatter are filled. This implies that the mean free path for nucleon motion is quite long, and a single-particle model is worth exploring.

One obvious and important characteristic of odd-$A$ nuclei is their ground-state spins and parities. Starting with the lightest nuclei, the general order of odd-$A$ ground-state spins and parities is $1/2^+$ for

neutron and proton and after the strongly bound $^4$He $3/2^-$, $1/2^-$ then, after $^{16}O_8$, it becomes $5/2^+$, $3/2^+$, $1/2^+$ and then, after $^{40}Ca_{20}$, $7/2^-$, $5/2^-$, $3/2^-$, $1/2^-$ an order reminiscent of the atomic shells in which the alternating parities are related to the orbital angular momentum suggesting a sequence: s-p-d and s-f and p to which a spin one-half is coupled. To obtain a model with such an ordering of angular momentum $l$-values requires solving a single-particle Schrodinger equation with a reasonable potential function. The form of this potential is not too important because only minor changes in $l$-value order occur using one or another $r$ dependence. The two simplest to calculate are the isotropic harmonic oscillator and the infinite square well. The latter is not realistic because the nucleon separation energy is quite finite and well-known for most nuclei. (One might also consider a potential function related to the charge distributions of Eqs. (1.16) and (1.19); however, these would require extensive numerical computing to extract the eigenvalues.) The angular momentum order of the levels and the number of particles in each for the isotropic harmonic oscillator is 1s (2); 1p (6), 1d, 2s (12); If, 2p (20); lg, 2d, 3s (30); and so on. (The semicolons separate the levels with different quanta of energy $\hbar\omega$, and most are degenerate.) The total number of levels thus becomes 2, 8, 20, 40, 70, 112, 168, which only agrees with the lowest observed ''magic numbers'' 2, 8, 20, 28, 50, 82, and 126 (cf. Section 1.6.1).

It took the genius of Maria Goeppert Mayer [35] and others [36] to realize that by adding a spin–orbit term of the form

$$V_{ls} = -V(r)\,\vec{l}\cdot\vec{s} \tag{1.59}$$

the theoretical order could be brought into agreement with that observed. The minus sign guarantees that the $j = l + 1/2$ level will lie below the $j = l - 1/2$ level, as observed and the dependence on $l$ makes that the effect increases with $l$ leaving the shell closures at 2, 8, 20 unaffected while introducing a new shell closure at 28 due to the lowering of the $1f_{7/2}$ orbit. Further, the observed closures at 50, 82, 126, are obtained in a natural way. Also the spins of the odd-$A$ ground states is mostly correctly predicted. The shell model explains via large gaps between the single-particle orbital energies the large binding energies of nuclei having $Z$ or $N$ a magic number making the number of stable isotopes/isotones particularly large, for example, there are 10 stable Sn isotopes with $Z = 50$. For the excited states, magic nuclei show them at very high excitation energies as one needs to break the closed shell and lift one particle over the large shell gap. As an example in the doubly magic nucleus $^{208}$Pb, an energy of 2.6 MeV is needed to create the first excited $3^-$ state and even 4.085 MeV for the $2^+$ state.

The robustness of double-magic nuclei allows a major truncation for shell model calculations. It turns out that they can in first instance be treated as inert cores, whereby the spins of all of the particles in the core pair off to zero. Thereby, only the so-called valence nucleons need to be considered. This is of importance as with increasing number of nucleons and possible orbitals, the shell model allows for many different configurations. As angular momentum and parity are conserved, the residual interaction used can be diagonalized separately for a given spin and parity. Nevertheless, the dimensions become quickly huge.

Although the shell model is one of the older nuclear models, it has become of increasing use in the last decades. This is due to two key aspects. The first is

the tremendous increase in computing power allowing large-scale shell model codes to be developed, including quantum Monte Carlo diagonalization. The second is the construction of effective *in medium* interactions starting from the nucleon–nucleon scattering data. Hereby the elimination of the hard core repulsion of the nucleon–nucleon interaction was crucial and produced a universal, so-called $V^{\text{low-}k}$ interaction. The recent progress opens the direct way from quantum chromodynamics (QCD) to the effective interactions, which is in particular very much needed for the study of exotic nuclei. The most involved calculations are done for light nuclei up to $^{11}$B. Here no-core shell model calculations are able to describe accurately binding energies and excited states for very light nuclei [37].

### 1.7.3 The Deformed Shell Model

As the very large quadrupole moments of the nuclei in the middle of the higher shells cannot be explained by the simple spherical model, their explanation requires large contributions from the even–even core, which carries all (or almost all) of the charge. It can be shown that a single-particle moving in a nonrigid potential well will have a lower energy if the well is not spherical, rather than if it is spherical. As the lowering of the particle energy is proportional to the eccentricity, such a system will assume a deformed equilibrium shape. The nuclear Hamiltonian will now contain a term that produces deviations from spherical:

$$H = H_0 + H_{\text{d}} - V_{\text{ls}}(r) + \text{cl}^2 \qquad (1.60)$$

where $H_0$ is the isotropic harmonic oscillator Hamiltonian and $V_{\text{ls}}(r)$ is the spin–orbit term, both of which have proved so successful for the spherical-shell model. (The $I^2$ term helps give the proper level order in the isotropic limit.) Expanding the nuclear surface in spherical harmonics gives

$$S(\theta,\phi) = R_0\left[a_0 + \sum_{\lambda>1,\mu} a_{\lambda\mu} Y_{\lambda\mu}(\theta,\phi)\right] \qquad (1.61)$$

where $R_0$ is the radius of the spherical nucleus and $a_0$ is unity to quantities of second order and assures that the volume remains constant for small deformations. Taking the lowest order, one has that

$$S(\theta,\phi) = R_0\left[1 + \sum_{-2}^{+2} a_{2\mu} Y_{2\mu}(\theta,\phi)\right] \qquad (1.62)$$

[This expression should be compared with the nuclear charge distribution of Eq. (1.19).] It is customary to take only the symmetric term $a_{20}$ in this equation to be nonzero. This then leads to the deformation term in the Hamiltonian

$$H_{\text{d}} = -Ka_{20}\omega_0^2 r^2 Y_{20}(\theta,\phi) \qquad (1.63)$$

The full Hamiltonian can now be diagonalized using a set of spherical shell model basis states, and the resulting deformed, single-particle states are called *Nilsson* states after Sven Gosta Nilsson [38], who first carried out this diagonalization. The operators in Eq. (1.60) do not connect oscillator states differing by one principal oscillator quantum number, $N$, but do connect states differing by two. Nilsson neglected matrix elements not diagonal in $N$. This is a reasonably good assumption as oscillator states differing by $N = 2$ are rather far apart, except for states belonging to large $N$ and large deformation (i.e.,

nuclei with large $A$ and large quadrupole moments). The Nilsson levels are labeled $\Omega|N,n_3,\Lambda]$. The symbol $\Omega$ is the projection of the particle angular momentum $j$ on the three axes of the body-fixed axis system and is a good quantum number. In the limit of very large deformations, the single-particle energy is given by

$$E = \left(n_3 + \frac{1}{2}\right)\hbar\omega_3 + (n_\perp + 1)\hbar\omega_\perp \tag{1.64}$$

where the symbol $\omega_3$ is the oscillator frequency along the symmetry axis and the symbol $\omega_\perp$ is the oscillator frequency in the perpendicular directions. Thus, in the limit of very large deformations, one has $N = n_3 + n_\perp$. In this same limit, the projection of the orbital angular momentum on the symmetry axis becomes the last label,

$$N = \pm n_\perp, \pm n_\perp - 2, \ldots, \pm 1 \text{ or } 0 \tag{1.65}$$

This scheme is used to label not only the ground states of deformed nuclei but also the excited state rotational band heads. The level order will now be $L$, $L+1$, $L+2$, ..., as a result of core rotation, so that, when a level does not fit into this sequence, it must belong to a different single-particle band. One now proceeds to assign quantum numbers to the states by determining the odd-nucleon number; then, because the Nilsson energy levels are plotted against the core deformation, one assigns the deformation by finding that place where a Nilsson level appears with the measured ground-state spin. The next Nilsson level up should give the excited-band head, and so on. As an example, consider the nucleus $^{173}Lu_{102}$, which has a $7/2^+$ ground state. Following the procedure above, the appropriate level is the 7/2[404], with excited members $9/2^+$, $11/2^+$, $13/2^+$. Just above the $9/2^+$ level is a close doublet with spins $5/2^-$, $1/2^-$, which has been assigned to the 1/2[541] Nilsson level. The $3/2^-$ level belonging to this band lies above the $9/2^+$ state. This nonuniform order of a 1/2 band is an example of Coriolis coupling, which mixes the level order of $\Omega = 1/2$ bands.

### 1.7.4 Collective Models of Even–Even Nuclei

In Section 1.6.4.2, where the rotational-level structures of even–even nuclei were discussed, it was pointed out that the moments of inertia play a crucial role to describe the atomic nucleus as a rigid-body momental ellipsoid. Bohr [32] proposed a model of the momental ellipsoid and thus of deformed even–even nuclei and the cores of odd-$A$ and odd–odd nuclei. Several important assumptions were made in order to extract these moments of inertia. The first is that the nuclear core is incompressible, so that the nuclear density is constant. Second, the flow is assumed to be irrotational, so that a velocity potential exists and satisfies Laplace's equation. Finally, it must be assumed that the motion is such as to preserve the principal axis system. The moments of inertia for quadrupole deformations then are

$$\mathfrak{I}_k^2 = 4B_2\beta^2\sin^2\left(\gamma - \frac{2\pi}{3}k\right) \tag{1.66}$$

Here $B_2$ and $\beta$ are the quadrupole mass and deformation parameters, while $\gamma$ is an asymmetry parameter whose range is $0 \le \gamma \le \pi/6$. There are similar relations for other deformations such as octupole ($Y3$), hexadecapole ($Y4$), and so on. The Hamiltonian for this system is now

$$H_{\text{quad}} = \frac{1}{2}B_2(\dot{\beta}^2 + \beta^2\dot{\gamma}) + \frac{1}{B_2\beta^2}\sum_{k=1}^{3}\frac{L_k^2}{\sin^2\left(\gamma - \frac{2\pi}{k}\right)} + \frac{1}{2}C_2\beta^2 \tag{1.67}$$

If the system is not rigid, then the deformation and asymmetry parameters are no longer fixed, and the system can execute either deformation ($\beta$) vibrations or asymmetry ($\gamma$) vibrations, or both. The β-vibrational bands have angular momentum 0 – they are akin to molecular "breathing" modes – and the γ-vibrational bands have angular momentum 2. Thus, nuclei will exhibit ground-state bands where $n_\beta = 0$ and $n_\gamma = 0$, β-bands $n_\beta = 1$, $n_\gamma = 0$), γ-bands ($n_\beta = 0$, $n_\gamma = 1$), and higher order bands. Although the β-vibrations are the simplest, they are not really well established [39], much better established are γ-bands of which double excitations with $n_\gamma = 2$ are found in nature [40].

In his original paper, Bohr [32] argued that the nucleus would stabilize around $\gamma = 0$, so that the momental ellipsoid was symmetric (long and thin, cigarlike), while the surface itself was spheroidal. Then $\mathfrak{I}_3 = 0$. This leads to difficulties as Eq. (1.50) shows that the energy eigenvalues become infinite unless $K = 0$. Thus, the ground-state bands of even–even nuclei have $K = 0$, and the angular momentum sequence becomes 0, 2, 4, 6, ..., which is what is observed. These models automatically conform to the $A$ representation. Again, if the system is not rigid, against β-vibrations, there will be one or more β-bands above the ground-state rotational band that mimic the ground-state band in spin sequence, but because $<\beta^2>$ will be greater than for the ground state, the levels will be closer together.

Finally, in this model if $\gamma$ is not constant, γ-vibrations can arise with angular momentum 2. (One might think of these as equatorial bulges moving around the nuclear equator. They are akin to the well-known Jacobi ellipsoids of a self-gravitating, rotating fluid.) These γ-vibrations then produce a γ-band that is different in spin sequence from the β- and ground-state bands. This occurs because $K_\gamma = 2$, not 0. The γ-band sequence is 2, 3, 4, 5, .... There can be several γ-bands with different $K$ values and different spin sequences. The lowest one has $K_\gamma = 2$, while the next will have $K_\gamma = 0$ and 4, and so on.

It must be made clear that the Bohr model is only applicable for the low-lying positive-parity levels. The negative-parity levels belonging to the $B_1$ representation have moments of inertia that are considerably more complicated as they represent an octupole or pearlike shape.

An example of a well-developed rotational system is $^{154}Sm_{92}$ where $R4/2 = 3.25$. This nucleus has a well-developed ground-state rotational band with the spin sequence $0^+$, $2^+$, $4^+$, ..., $12^+$ with the first excited state rather low in energy at 81.99 keV. It has a β-band with a $0^+$ band head 1099.28 keV, followed by the first excited $2^+$ state at 1177.78 keV ($\Delta E = 78.52$ keV). This is a striking example of the increase in the moment of inertia due to the quantum of β-vibrational energy. Furthermore, the $K = 2$ γ-band, with sequence $2^+$, $3^+$, $4^+$, ..., starts at 1440.05 keV.

Also to be seen is an octupole band starting with the $1^-$ level at 921.39 keV, followed by the $2^-$, $3^-$, $5^-$, ... in the expected order. Thus, one sees four well-developed rotational bands fitting quite nicely into the model scheme.

Further, the collective behavior manifests itself in the quadrupole moments and electric quadrupole transitions. The axially

symmetric core collective model yields for a state with quantum numbers $K$ and $I$ a laboratory quadrupole moment $Q$:

$$Q = \frac{3K^2 - I(I+1)}{(I+1)(2I+3)} Q_0 \tag{1.68}$$

with an intrinsic quadrupole moment $Q_0$ given by

$$Q_0 = \frac{3}{\sqrt{5\pi}} Z R_0^2 \beta (1 + 0.16\beta) \tag{1.69}$$

The fact that by definition $K$ has to be lower than $I$ (Eq. (1.74)) produces almost always a change of sign between intrinsic and laboratory quadrupole moments. Related to the intrinsic quadrupole moments are the $B(E2)$ values. In between states belonging to a given $K$ band, they are given by

$$B(E2; I_i \rightarrow I_f) = \frac{5}{16\pi} e^2 Q_0^2 \left\langle I_i K 20 | I_f K \right\rangle^2 \tag{1.70}$$

When comparing Eq. (1.70) directly with the data, one often extracts the transition quadrupole moment $Q_t$ as being the $Q_0$ value obtained for a given transition. A very useful relation is obtained for $B(E2)$ ratios between states belonging to bands having different $K$ quantum numbers. These relations are called the *Alaga rules* and yield

$$\frac{B(E2; I_i \rightarrow I_f)}{B(E2; I_i \rightarrow I'_f)} = \left( \frac{\left\langle I_i K 2 \Delta K | I_f K_f \right\rangle}{\left\langle I_i K 2 \Delta K | I'_f K_f \right\rangle} \right)^2 \tag{1.71}$$

whereby $\Delta K = K_f - K$ as is expected for an angular momentum projection quantum number. Using the Alaga rules it is possible to determine the $K$ values of rotational bands.

If one does not follow the Bohr assumption that the nucleus will stabilize around $\gamma = 0$ but around some other value within its range, then one has to deal with an asymmetric rotator, which will have a considerably more complicated eigenvalue structure. Davydov and Filippov [41] made an extensive investigation and showed that one obtained better results with such a model than with a symmetric one. However, one loses the computational simplicity of the symmetric model.

### 1.7.5 Boson Models

The models discussed up until now and that have been used most extensively would seem to be almost mutually exclusive. The shell model and its modifications, such as Nilsson's extension to a deformed system, focus on the single-particle aspects of nuclear structure. On the other hand, the collective model of Bohr and Mottelson, and extensions, place the emphasis on the cooperative, or fluid, aspects of these systems. Thus, they seem to stand apart and be almost unrelated. This has led to the next step, the investigation of models that are called *microscopic models* or *calculations*. These include pairing models (similar to the Bardeen–Cooper–Schriefer theory of superconductivity) and the random-phase approximation, to name but two. A more recent and still developing set of microscopic models is called the *interacting boson models*, which we present here briefly.

The solutions of the nuclear shell model lead to single-particle orbits that can be occupied by the neutrons and protons. Because of the Pauli principle, each nucleon in an atomic nucleus can occupy only different orbits. It turns out that once more the short range of the nuclear force leads to a dominant component when

one wants to take account of the residual interaction. The dominant component is called *pairing interaction* and energetically favors the formation of nucleon pairs made out of two nucleons moving in orbits |njm> and |nj-m>, coupling to a two-nucleon state with total spin $J=0$. To a lesser extent, the formation of nucleon pairs with spin $J=2$, 4, 6 in that sequence is also favored. As the number of protons and neutrons is generally different in not too light nuclei, the single-particle orbits occupied by both will generally be very different and thus the pairing will be effective only between like nucleons (either protons or neutrons). When one is mainly interested in the low-energy excitations of the atomic nucleus, one can treat this structure in terms of interacting, nucleon pairs via the residual interaction. However, a many-body problem composed of paired fermions, although more correct, is still very difficult to solve. Instead by replacing these $n=n_\nu+n_\pi$ fermions by

$$N=\frac{n_\nu+n_\pi}{2} \tag{1.72}$$

real bosons with $L=0$, 2 (and eventually 4, 6, ...), one has enormously simplified the original $n$-body problem. For instance, one does not need to bother about which orbits are occupied by the protons and neutrons, while keeping the essential physics. This is the essence of what is now called the *interacting boson approximation*, which was proposed and elaborated by Iachello and Arima in the second half of the 1970s [42].

The simplest version of the model is called *IBM-1* and deals with s ($L=0$) and d ($L=2$) bosons. Considering the constraint that the number of bosons is fixed $N=n_\mathrm{s}+n_\mathrm{d}$ and limiting the Hamiltonian to one- and two-body interactions, one obtains the multipole expansion form

$$\begin{aligned}\widehat{H}=\varepsilon\widehat{n}_d+c_1\widehat{L}\cdot\widehat{L}+c_2\widehat{Q}\cdot\widehat{Q}\\ +c_3\widehat{T}_3\cdot\widehat{T}_3+c_4\widehat{T}_4\cdot\widehat{T}_4\end{aligned} \tag{1.73}$$

with the operators

$$\widehat{L}_m=\sqrt{10}(d^\dagger\times\widetilde{d})^{(1)}_m \tag{1.74a}$$

$$\begin{aligned}\widehat{Q}_m=\;&(s^\dagger\times\widetilde{d}+d^\dagger\times s)^{(2)}_m\\ &+\chi(d^\dagger\times\widetilde{d})^{(2)}_m\end{aligned} \tag{1.74b}$$

$$\widehat{T}_{3m}=(d^\dagger\times\widetilde{d})^{(3)}_m \tag{1.74c}$$

$$\widehat{T}_{4m}=(d^\dagger\times\widetilde{d})^{(4)}_m \tag{1.74d}$$

The factor $\sqrt{10}$ is used in order to make the dipole operator an angular momentum operator and the first term in Eq. (1.73) contains the d-boson number operator. The multipole expansion has six free parameters of which two are needed for the quadrupole–quadrupole interaction. The use of the multipole expansion is especially advantageous because numerical studies have shown that the values of the octupole and hexadecapole interaction are generally very small. Thus, up to a good approximation, one can describe a variety of atomic nuclei at low excitation energies by the simple four-parameter Hamiltonian:

$$\widehat{H}^\chi=\varepsilon\widehat{n}_d+c_1\widehat{L}\times\widehat{L}+c_2\widehat{Q}^\chi\times\widehat{Q}^\chi \tag{1.75}$$

The index in Eq. (1.75) makes explicit that the quadrupole operator contains an additional parameter.

Of importance in the development of the IBM is the use of dynamical symmetries providing analytic solutions of the many-body problem. Because there are in total six distinct bosons when considering the magnetic projections, the symmetry of the many-body problem is $U(6)$ while the physical symmetry is given by SO(3) the Lie algebra of the angular momentum. Three

dynamical symmetries are obtained. They can be schematically represented by the chains

$$U(6)\left\{\begin{array}{l}\supset U(5)\\ \supset O(6)\\ \supset SU(3)\end{array}\right\}\quad\left.\begin{array}{l}\\ \supset O(5)\\ \\ \end{array}\right\}\supset O(3) \tag{1.76}$$

Each of the three chains can be used to provide a complete basis to analytically solve the $N$ s, d boson model. One can also rewrite the general Hamiltonian as a combination of all previously determined Casimir operators:

$$\begin{aligned}\widehat{H} = {} & \varepsilon C_1[U(5)] + \alpha C_2[U(5)] \\ & + \delta C_2[SU(3)] + \eta C_2[O(6)] \\ & + \beta C_2[O(5)] + \gamma C_2[O(3)]\end{aligned} \tag{1.77}$$

where we have omitted all constant terms that contribute only to the binding energies. The Casimir form Eq. (1.77), like Eq. (1.73), contains six parameters and, once more, all three forms can be transformed into each other. The advantage of the form Eq. (1.77) lies in the fact that the three different limits correspond to three classes of atomic nuclei: vibrational, rotational, and $\gamma$-unstable nuclei correspond to the Hamiltonian with $\delta = \eta = 0$ ($U(5)$ limit), $\varepsilon = \alpha = \eta = \beta = 0$ (SU(3) limit) and $\varepsilon = \alpha = \delta = 0$ ($O(6)$ limit) . In these cases, closed analytic expressions for excitation energies and wavefunctions can be obtained [42]. Two of the limits already had known counterparts in the collective model. It was the discovery of the third, the $O(6)$ limit, in the Pt nuclei at the end of the 1970s [43], that boosted the use of the model. Soon it became evident that it formed a good approximation for the nuclear many-body problem in many nuclei. Outside the limits the model needs to be solved numerically and the transitional nuclei can be described.

The IBM-1 model describes only positive-parity levels of even–even nuclei. To describe negative-parity states, one must use negative parity p and f bosons constructed in a similar way to the s and d bosons. Furthermore, the IBM-1 has no explicit neutron–proton degree of freedom. This is introduced in the IBM-2 where a neutron–proton label is introduced for the s and d bosons. As the neutron and proton bosons are distinguishable, the IBM-2 leads to new sets of states, called *mixed symmetry states* (in the neutron–proton degree of freedom). Furthermore, analytical solutions can be derived for the IBM-2 [44]. Mixed symmetry states have been observed in many atomic nuclei, especially in deformed nuclei where the lowest state is a $1^+$ state called the *scissor state* [45], and also recently in vibrational nuclei [46].

Finally, if one wants to describe odd-$A$ nuclei, a model denoted interacting boson–fermion model (IBFM) must be used. Odd-$A$ nuclei always have an unpaired nucleon that cannot form an s or d boson because a partner is missing. Therefore, an odd–even nucleus is described in the model with $N$ bosons and one fermion, the unpaired nucleon, which can occupy several orbitals $j$. In addition, for such systems dynamical symmetries, called *Bose–Fermi symmetries*, can be used, although their elaboration is much more complex [47]. The symmetry starts then from the product $U^{\mathrm{B}}(6) \times U^{\mathrm{F}}(M)$ with

$$M = \sum_j 2j + 1 \tag{1.78}$$

and ends with SU(2). In 1980, a daring extension of the model was proposed [48]. Using supersymmetry, the structure of some odd–even nuclei could be related

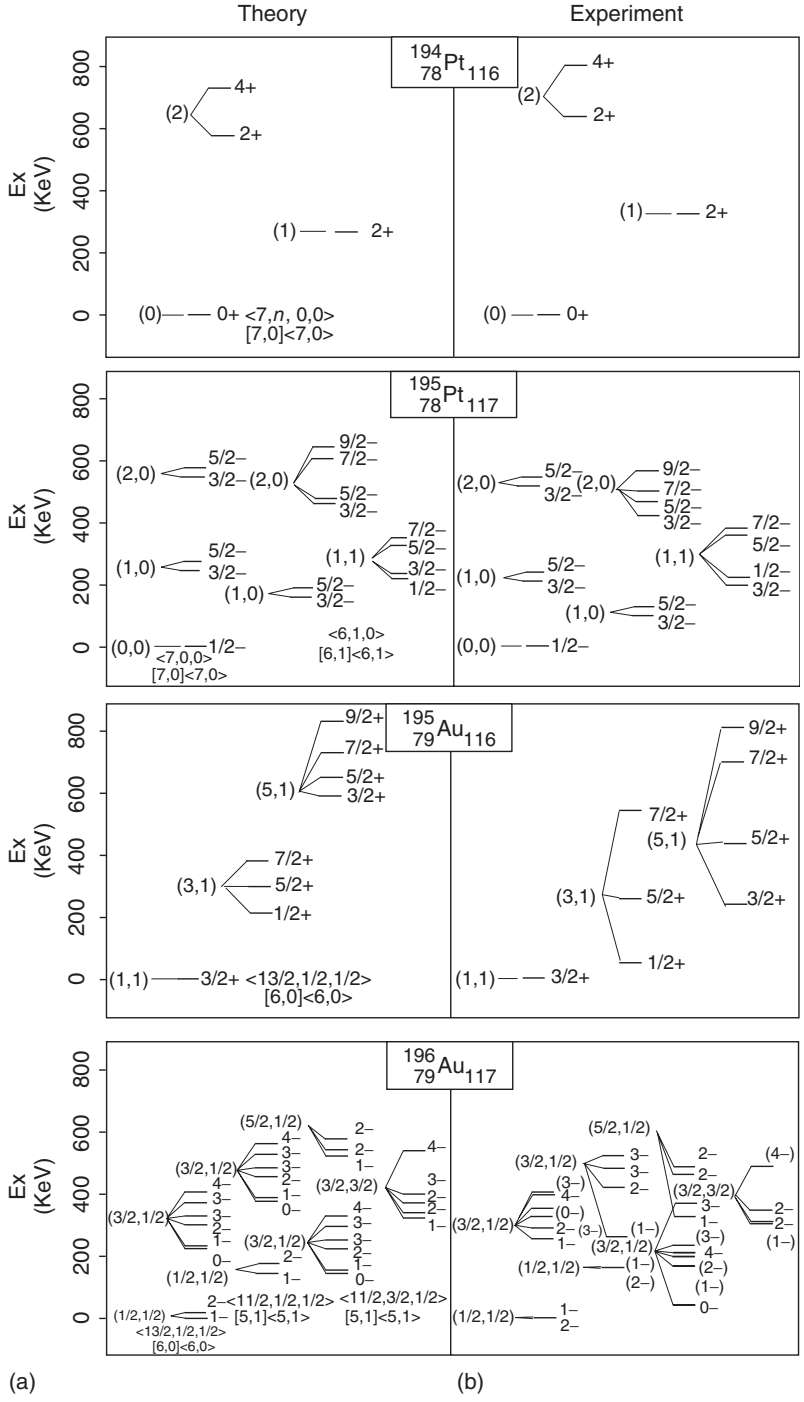
Theory
Experiment
194 78 Pt 116
195 78 Pt 117
195 79 Au 116
196 79 Au 117
Ex (KeV)
0
200
400
600
800
(a)
(b)

to that of the much simpler even–even nuclei via the embedding of the dynamical symmetries in a supersymmetry:

$$\begin{array}{ccccc} U(6/M) & \supset & U^{\mathrm{B}}(6) & \times & U^{\mathrm{F}}(M) \\ | & & | & & | \\ [N] & & [\mathrm{N}] & & [1^m] \end{array} \qquad (1.79)$$

connecting the N s, d bosons + 1 fermion problem to the N + 1 boson problem by the supersymmetric reduction rule $N = \mathrm{N} + m$. This embedding when realized in nature would reveal itself through the possibility to describe excited states in an odd–even nucleus and in the adjacent even–even nuclei using a common set of quantum numbers and parameters related via the supergroup. If dynamical symmetries are required, only a limited class of atomic nuclei can be described in this way. During the 1980s, experimental evidence was accumulated, but unfortunately it was not possible to determine completely the structure of the odd–even nucleus starting from the even–even nucleus alone.

Later an extension of supersymmetry was proposed, which incorporates a distinction between neutrons and protons. This extended supersymmetry allows one to describe a quartet of nuclei in a common framework. This quartet, called a *magic square*, consists of nuclei having the same total number of bosons (paired nucleons) and fermions (unpaired nucleons). It consists of an even–even nucleus, two odd–even nuclei and an odd–odd nucleus. The latter is interesting in two respects: its energy spectrum can be predicted from those of the other three members and heavy odd–odd nuclei are the most complex objects found in low-energy nuclear structure. If dynamical supersymmetry is able to describe these nuclei, which could not be described by other theoretical models, strong evidence for its existence can be obtained. This development is of importance not only for nuclear physics but for all other applications of supersymmetry in physics.

The odd–odd nucleus $^{196}$Au is considered to be the ultimate test of supersymmetry in nuclear physics for three reasons. It is situated in a region of nuclei that was known to exhibit dynamical symmetries and supersymmetries. At the same time, it is the most difficult mass region in which to describe odd–odd nuclei. Finally, when its excitations with negative parity were predicted in 1989 on the basis of the three other nuclei, none of them were experimentally known. In a detailed spectroscopic study the excited states of $^{196}$Au were determined and a good agreement with the supersymmetric model was obtained [49]. The results of this combined effort are illustrated in Figure 1.6. They reveal good agreement with the analytical prediction:

**Figure 1.6** The lowest observed states (b), are compared to the theoretical result (a) for the four members of the quartet (note that one is dealing with holes in the doubly closed shell nucleus $^{208}$Pb). The even–even nucleus $^{194}$Pt, the negative parity states in the odd-neutron nucleus $^{195}$Pt, the positive parity states in the odd-proton nucleus $^{195}$Au and the negative-parity states in the odd–odd nucleus $^{196}$Au up to 500 keV can be described using the formula (Eq. (1.88)) based on dynamical supersymmetry. Not shown are higher-lying states of the even–even and odd–even nuclei, which are also described by supersymmetry. Together with the spin and parities, the quantum numbers $[N_1,N_2]$, $<\Sigma_1,\Sigma_2>$, $<\sigma_1,\sigma_2,\sigma_3>$, and $(\tau_1,\tau_2)$ are also indicated. (Based on [49].)

$$
\begin{aligned}
E = {} & A(N_1(N_1+5) + N_2(N_2+3)) \\
& + B(\Sigma_1(\Sigma_1+4) + \Sigma_2(\Sigma_2+2)) \\
& + B'(\sigma_1(\sigma_1+4) + \sigma_2(\sigma_2+2) + \sigma_3^2) \\
& + C(\tau_1(\tau_1+3) + \tau_2(\tau_2+1)) \\
& + DL(L+1) + EJ(J+1) \qquad (1.80)
\end{aligned}
$$

obtained using dynamical supersymmetry.

## Glossary

**Bosons:** Quantum particles obeying Bose–Einstein statistics, so having integral spin.

**Daughter:** In a radioactive decay in which the radioactive nucleus A decays into nucleus B the nucleus B is said to be the daughter of nucleus A.

**de Broglie wavelength:** The wavelength $\lambda$ of a particle given by the relation $\lambda = hp$, where $h$ is Planck's constant and $p$ the momentum of the particle.

**Decay constant $\lambda$:** If $N$ nuclei are present at time $t$, then the decay constant is given by the number of decaying nuclei $-\mathrm{d}N/\mathrm{d}t$ divided by N.

**Electron capture:** A radioactive decay process, sometimes called *K capture*, where the decay energy $Q$ is greater than the binding energy of one of the atom's cloud of electrons ($Q > BEe$). The nucleus absorbs one of the atomic electrons to undergo $\beta^+$ decay and emits thereby a neutrino. If $Q > 2m_e c^2$, then electron capture competes with normal $\beta^+$ decay, whereby a positron and an electron neutrino are created.

**Fermions:** Half integer spin particles obeying Fermi–Dirac statistics.

**Half-life $T_{1/2}$:** In radioactive decay, the time in which half of the nuclei initially present decay.

**Isobars:** Nuclei with the same mass number $A$ but with different numbers of protons ($Z$) and neutrons ($N$).

**Isomeric state:** An excited nuclear state whose half-life for $\gamma$-emission is quite long; similar to a metastable state of an atomic system.

**Isotones:** Nuclei with the same number of neutrons ($N$) but different numbers of protons ($Z$) and thus, different values for $A$.

**Isotope shift:** Small changes in the wavelengths of X-ray optical, and especially muonic transitions in going from one isotope to the next, which give a measure of the change in the nuclear radius as $A$ changes by one unit.

**Isotopes:** Nuclei with the same number of protons ($Z$) but different numbers of neutrons ($N$) and thus, different values of $A$.

**Lamb shift:** A small quantum electrodynamic effect that is principally due to the radiative coupling of the orbiting electron (or muon) with the vacuum field and the finite nucleus.

**Lifetime $\tau$:** The reciprocal of the decay constant. The lifetime is related to the half-life by $T_{1/2} = \ln(2)\tau$.

**Mass defect:** The difference between the mass of a nucleus of mass number $A$ in atomic mass units less $A$, $\Delta = M(A) - A$.

**Mass excess:** Negative of *mass defect*.

**Mirror pair:** Two light nuclei with the same mass number $A$ but with numbers of protons ($Z$) and neutrons ($N$) interchanged.

**Muon:** A member of the lepton family of elementary particles with spin one-half. The muon is 207 times as heavy as an electron and has a lifetime of

$2.197 \times 10^{-6}$ s. The muon, like the electron, has a negative charge.

**Nuclear polarization:** A small reduction in the Coulomb potential caused by the penetration of the nuclear volume by the bound orbiting particle (an electron or muon).

**Packing fraction:** The mass defect per unit mass number $P = \Delta/A$.

**Parity $\pi$:** The behavior of a state function upon reflection of the coordinates through the origin, $r \rightarrow -r$, then either $\phi(-r) = +\phi(r)$ and the state is said to have *positive parity* or $\phi(-r) = -\phi(r)$ and the state is said to have *negative parity*.

**Pauli principle:** The requirement that in a system of like particles obeying Fermi–Dirac statistics (half integer spin particles), no two particles can have the same set of quantum numbers. More generally, the Pauli principle requires wavefunctions for identical particles to be antisymmetric for fermions and symmetric for bosons upon interchange of two particles.

**Phonon:** In nuclear physics a phonon is a quantized surface vibration of a quantum fluid.

**Vacuum polarization:** A small radiative correction to the Coulomb potential of an atom arising from the emission and reabsorption of virtual positron–electron pairs.

**Valley of stability:** In a three-dimensional plot of the nuclear masses $M(Z,N)$ with the proton number $Z$ as abscissa neutron number $N$ as ordinate and $M(Z,N)$ normal to the $Z$–$N$-plane, the stable nuclei will be found along a region where $N \sim Z$, which appears to form a deep valley – *the valley of stability*.

**Woods–Saxon potential:** For a real potential function, this is written with an adjustable surface diffuseness parameter and a radius parameter $R$. For a complex potential, one adds a similar term, $V_{\mathrm{Im}}$.

## References


1. Rutherford, E. (1911) *Philos. Mag.*, **21**, 669–688.
2. Moseley, H.G.J. (1913) *Philos. Mag.*, **26**, 1024–1034.
3. Moseley, H.G.J. (1914) *Philos. Mag.*, **27**, 703–713.
4. Soddy, F. (1913) *Nature*, **92**, 399–400.
5. Rutherford, E. (1919) *Philos. Mag.*, **37**, 581–586.
6. Harkins, W.D. and Majorsky, S.L. (1922) *Phys. Rev.*, **19**, 135–156.
7. Pauli, W. (1924) *Naturwissenschaften*, **12**, 741–743. reprinted in Kronig, R., Weisskopf, V. F. (eds) (1964) *Collected Scientific Papers*, Vol. 2, New York: John Wiley & Sons, Inc., pp. 198–200.
8. Racah, G. (1931) *Z. Phys.*, **71**, 431–434.
9. Chadwick, J. (1932) *Nature*, **129**, 312.
10. Heisenberg, W. (1932) *Z. Phys.*, **77**, 1.
11. Bethe, H.A. and Bacher, R.F. (1936) *Rev. Mod. Phys.*, **8**, 82–229.
12. Bethe, H.A. (1937) *Rev. Mod. Phys.*, **9**, 69–244.
13. Avignone, F.T. III, Elliott, S.R., and Engel, J. (2008) *Rev. Mod. Phys.*, **80**, 481–516.
14. Lederer, C.M. and Shirley, V.S. (eds) (1978) *Table of Isotopes*, 7th edn, John Wiley & Sons, Inc., New York.
15. Kudomi, N., Ejiri, H., Nagata, K., Okada, K., Shibata, T., Shima, T., and Tanaka, J. (1992) *Phys. Rev.*, **46**, R2132–R2135.
16. Bohr, A. and Mottelson, B. (1969) *Nuclear Structure*, Vol. I, Benjamin, New York.
17. Myers, W.D. and Swiatecki, W.J. (1966) *Nucl. Phys.*, **81**, 1–60.
18. Myers, W.D. (1977) *Droplet Model of Atomic Nuclei*, IFI/Plenum, New York, and references therein.
19. Möller, P., Nix, J.R., Myers, W.D., and Swiatecki, W.J. (1995) *Atomic Data Nucl. Data Tables*, **39**, 185–225.
20. Duflo, J. and Zuker, A.P. (1995) *Phys. Rev. C*, **52**, R23–R27.
21. Goriely, S., Samyn, M., and Pearson, J.M. (2007) *Phys. Rev. C*, **75**, 064312.

22. Lunney, D., Pearson, J.M., and Thibault, C. (2003) *Rev. Mod. Phys.*, **75**, 1021–1082.
23. de Vries, H., de Jager, C.W., and de Vries, C. (1987) *Atomic Data Nucl. Data Tables*, **36**, 495–536.
24. Tanihata, I. (1995) *Prog. Part. Nucl. Phys.*, **35**, 505–574.
25. Casimir, H.B.G. (1935) *Physica*, **2**, 719–723.
26. Gollnow, G. (1936) *Z. Phys.*, **103**, 443–453.
27. Schwartz, C. (1955) *Phys. Rev.*, **97**, 380–395.
28. Castel, B. and Towner, I.S. (1990) *Modern Theories of Nuclear Moments*, Clarendon Press: Oxford, and references therein.
29. Neyens, G. (2003) *Rep. Prog. Phys*, **66**, 633–689.
30. Eberth, J. and Simpson, J. (2008) *Prog. Part. Nucl. Phys.*, **60**, 283–337.
31. Heyde, K.L.G. (1990) *The Nuclear Shell Model*, Springer Series in Nuclear and Particle Physics, Springer(A).
32. Bohr, A. (1952) *Kgl. Dan. Vid. Selsk. Mat. Fys. Medd.*, **26** (14).
33. Jolie, J., Cejnar, P., Casten, R.F., Heinze, S., Linnemann, A., and Werner, V. (2002) *Phys. Rev. Lett.*, **89**, 182502.
34. Cejnar, P., Jolie, J., and Casten, R.F. (2010) *Rev. Mod. Phys.*, **82**, 2155–2212.
35. See also: Mayer, M. G. (1948) *Phys. Rev.* **74**, 235–239; *Phys. Rev*, (1949), **75**, 1969–1970.
36. Haxel, O., Jensen, J.H.D., and Suess, H.E. (1949) *Phys. Rev.*, **75**, 1766.
37. Pieper, S.C., Varga, K., and Wiringa, R.B. (2002) *Phys. Rev.*, **C66**, 044310.
38. Nilsson, S.G. (1955) *Kgl. Dan. Vid. Selsk. Mat. Fys. Medd.*, **29**, 16.
39. Garrett, P.E. (2001) *J. Phys.*, **G27**, R1.
40. Börner, H.G. *et al.* (1991) *Phys. Rev. Lett.*, **66**, 691 and 2837.
41. Davydov, A.S. and Filippov, G.F. (1958) *Nucl. Phys.*, **8**, 237–249.
42. Iachello, F. and Arima, A. (1987) *The Interacting Boson Model*, Cambridge University Press, Cambridge.
43. Casten, R.F. and Cizewski, J.A. (1978) *Nucl. Phys.*, **A309**, 477.
44. Van Isacker, P., Heyde, K., Jolie, J., and Sevrin, A. (1986) *Ann. Phys.*, **171**, 253–296.
45. Richter, A. (1995) *Prog. Particle Nucl. Phys.*, **34**, 261.
46. Pietralla, N., von Brentano, P., and Lisetskij, A.G. (2008) *Prog. Particle Nucl. Phys.*, **60**, 225–282.
47. Iachello, F. and Van Isacker, P. (1991) *The Interacting Boson-Fermion Model*, Cambridge University Press, Cambridge.
48. Iachello, F. (1980) *Phys. Rev. Lett.*, **44**, 772–775.
49. Groeger, J. *et al.* (2000) *Phys. Rev. C*, **62**, 064304.


## Further Readings

In this list, the symbols E, I, and A following the references indicate the level of difficulty: elementary, intermediate, and advanced, respectively.


Bethe, H.A. (1936) *Rev. Mod. Phys.*, **8**, 82–229 (I).
This and the preceding form the best review of the early state of the subject: Bethe, H.A. and Bacher, R.F. (1937) *Rev. Mod. Phys.*, **9**, 69–244(I).
Bohr, A. and Mottelson, B. (1969) *Nuclear Structure*, Vol. 1, Benjamin, New York(A).
This and the preceding, while old, are comprehensive and still useful:
Bohr, A. and Mottelson, B. (1975) *Nuclear Structure*, Vol. 2, Benjamin, New York(A).
Bonatsos, D. (1988) *Interacting Boson Models of Nuclear Structure*, Clarendon, Oxford(A).
Castel, B. and Towner, I.S. (1990) *Modern Theories of Nuclear Moments*, Clarendon, Oxford(A).
An excellent text, more advanced than Pal (1983):
Casten, R.F. (1990) *Nuclear Structure from a Simple Perspective*, Oxford University Press, New York(I).
An overview of the use of symmetry concepts in nuclear structure with many experimental examples:
Frank, A., Jolie, J., and Van Isacker, P. (2008) *Symmetries in Atomic Nuclei: From Isospin to Supersymmetry*, Springer Tracts in Modern Physics, Springer (A).
A nice introduction into the practical aspects of the nuclear shell model:
Heyde, K.L.G. (1990) *The Nuclear Shell Model*, Springer Series in Nuclear and Particle Physics, Springer (A).
An excellent introduction for students of which each new edition is substantially updated:
Heyde, K.L.G. (1994) *Basic Ideas and Concepts in Nuclear Physics*, Fundamental and Applied Nuclear Physics, IOP (I).

Discusses many aspects, both theoretical and experimental, of this fascinating area of nuclear structure:
Janssens, R.V.F. and Khoo, T.L. (1991) Superdeformed nuclei. *Annu. Rev. Nucl. Part. Sci.*, **41**, 321–355 (A).

An ideal textbook for students:
Krane, K.S. (1987) *Introductory Nuclear Physics*, John Wiley & Sons, Inc., New York (I).

A compendium of nuclear data, of great value:
Lederer, C.M. and Shirley, V.S. (eds) (1978) *Table of Isotopes*, 7th edn, John Wiley & Sons, Inc., New York (A).

Nice treatments of several of the older microscopic models:
Pal, M.K. (1983) *Theory of Nuclear Structure*, Van Nostrand Reinhold, New York (E).

Very deep and detailed introduction in the algebraic methods used in the nuclear shell model and the interacting boson model:
Talmi, I. (1993) *Simple Models of Complex Nuclei, Contemporary Concepts in Physics*, Harwood Academic Publishers, Chur (A).

Another excellent, more advanced text:
Wong, S.S.M. (1990) *Introductory Nuclear Physics*, Prentice-Hall, Englewood Cliffs, NJ (I).